



HAL
open science

Identification of a new series of flavopiridol-like structures as kinase inhibitors with high cytotoxic potency

Nada Ibrahim, Pascal Bonnet, Jean-Daniel Brion, Jean-François Peyrat, Jerome Bignon, H el ene Levaique, B eatrice Josselin, Thomas Robert, Pierre Colas, St ephane Bach, et al.

► To cite this version:

Nada Ibrahim, Pascal Bonnet, Jean-Daniel Brion, Jean-Fran ois Peyrat, Jerome Bignon, et al.. Identification of a new series of flavopiridol-like structures as kinase inhibitors with high cytotoxic potency. *European Journal of Medicinal Chemistry*, 2020, 199 (31), pp.112355. 10.1016/j.ejmech.2020.112355 . hal-03036489

HAL Id: hal-03036489

<https://hal.science/hal-03036489v1>

Submitted on 10 Dec 2020

HAL is a multi-disciplinary open access archive for the deposit and dissemination of scientific research documents, whether they are published or not. The documents may come from teaching and research institutions in France or abroad, or from public or private research centers.

L'archive ouverte pluridisciplinaire **HAL**, est destin ee au d ep ot et  a la diffusion de documents scientifiques de niveau recherche, publi es ou non,  emanant des  tablissements d'enseignement et de recherche fran ais ou  trangers, des laboratoires publics ou priv es.

Identification of a new series of Flavopiridol like structures as kinase inhibitors with high cytotoxic potency

Nada Ibrahim^a, Pascal Bonnet,^b Jean-Daniel Brion^a, Jean-François Peyrat^a, Jerome Bignon^c, Helene Levaique^c, Béatrice Josselin^{c,d}, Thomas Robert^{d,e}, Pierre Colas,^d Stéphane Bach^{d,e}, Samir Messaoudi^a, Mouad Alami^{a,*}, Abdallah Hamze^{a,*}

^aBioCIS, Equipe Labellisée Ligue Contre le Cancer, Univ. Paris-Sud, CNRS, University Paris-Saclay, F-92290, Châtenay Malabry, France

^bInstitut de Chimie Organique et Analytique (ICOA), UMR7311 Université d'Orléans-CNRS, Rue de Chartres, BP 6759, 45067, Orléans, Cedex 2, France

^cInstitut de Chimie des Substances Naturelles, UPR 2301, CNRS, F-91198, Gif sur Yvette, France

^dSorbonne Université, CNRS, UMR8227, Integrative Biology of Marine Models Laboratory (LBI2M), Station Biologique de Roscoff, 29680, Roscoff, France

^eSorbonne Université, CNRS, FR2424, Plateforme de criblage KISSf (Kinase Inhibitor Specialized Screening Facility), Station Biologique de Roscoff, 29680, Roscoff, France

Corresponding authors. Email: abdallah.hamze@u-psud.fr ; mouad.alami@u-psud.fr ;

Abstract

In this work, unique structure of flavopiridol analogs bearing thiosugars, amino acids and heterocyclic moieties tethered to the flavopiridol *via* thioether and amine bonds mainly on its C ring have been prepared. The analogs bearing thioether-benzimidazoles as substituents have demonstrated high cytotoxic activity *in vitro* against up to seven cancer cell lines. Their cytotoxic effects are comparable to those of flavopiridol. The most active compound (**13c**) found after the structure-activity relationship (SAR) showed the best antiproliferative activity and was more efficient than the reference compound. In addition, compound **13c** showed significant nanomolar inhibition against CDK9 and GSK3 β protein kinases.

Keywords: Favopiridol , cytotoxicity, Kinase inhibition, structure-activity relationship.

Highlights

- Twenty-two new analogs of flavopiridol were synthesized
- Five compounds showed high antiproliferative activity on seven cancerous cell lines
- Compound **13c** showed more cytotoxic potency than flavopiridol
- Compound **13c** showed a better selectivity for CDK9 and GSK3 β

1. Introduction

Flavones-based scaffolds belong to privileged family of bioactive structures.[1-4] This attribute is undoubtedly due to the enormous number of therapeutic benefits they exhibit. Particularly, in cancer diseases, flavonoids are known for their ability to inhibit important cell signaling proteins such as cyclin-dependent kinases (CDKs).[5-7] CDKs are well-known to be the main key regulators of cell cycle progression, their hyperactivation is associated with several cancers. For this reason, CDK inhibitors are of great importance to explore as novel therapeutic agents for cancer treatment.[8] CDK4/6 inhibitors have already reach the drug market (Palbociclib approved by FDA in 2015, Abemaciclib and Ribociclib both approved by FDA in 2017) for the treatment of advanced breast cancer treatment.[9] Earlier CDK inhibitors are described as purine derivatives and this is because they are ATP competitive ligands; for example dimethylaminopurine,[10] olomoucine[11] roscovitine[12-14] and other potent purine based CDK inhibitors.[15] Like purines, flavones have also shown their potency in disrupting cell cycle and have been thus demonstrated as potent CDK inhibitors.[16-18]

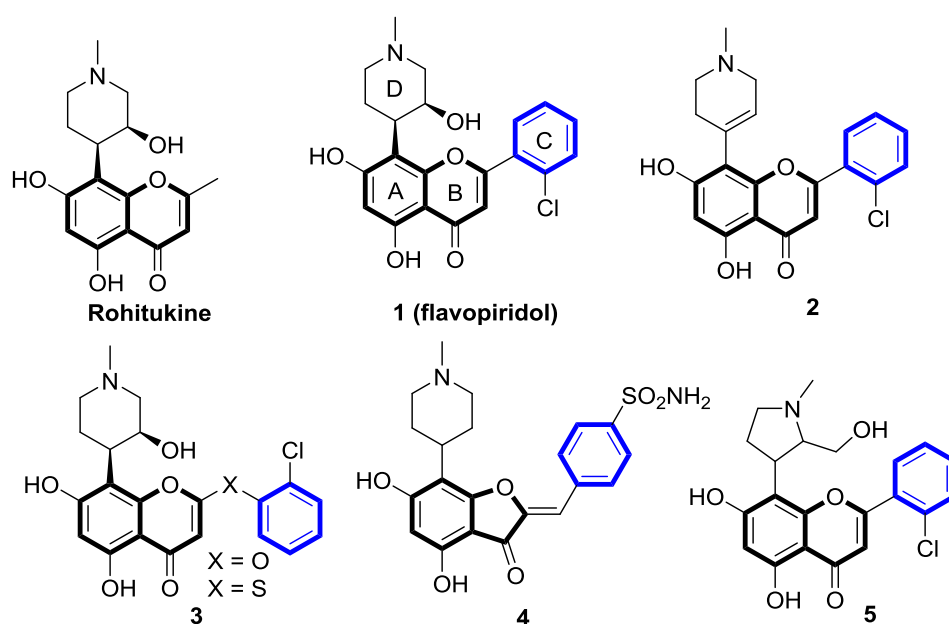


Figure 1. Flavopiridol and mimics as potent CDKs inhibitors

The seminal discovery of flavopiridol (alvocidib) **1** (Figure. 1) whose structure was inspired by the natural anti-rheumatic flavonoid “Rohitukine”[19-22] led to the development of new synthetic flavonoids-based compounds as inhibitors of kinases. Alvocidib, the first CDKs (CDK1, 2, 4, 6, 7, 9) inhibitor to be tested in a clinical trial[23-25] is the most active CDK9 inhibitor with IC₅₀ value of 20 nM. This drug is capable to induce regluated cell death with a block in the cell cycle at the G1/S and G2/M phases.[26-28] In 2004, it has received the Orphan Drug designation in chronic lymphocytic leukemia (CLL) from the FDA and the EMA respectively.[29, 30] The extensive amount of medicinal chemistry efforts has been reported on the study of flavopiridol, aiming to understand the mechanism of action and the structural modifications in order to discover new CDKs inhibitors.[31, 32] As a result of this research, P-276-00 (Piramal) a flavopiridol analogue has reached advanced stages of clinical development for cancer treatment.[33] Besides, previous SAR studies contributed to the identification of flavopiridol mimics (Figure 1) with selective inhibitory activity against CDK1 and 4, though with reduced potency. For example, the flavopiridol D-ring olefin analogue (**2**) was reported as a CDK4 selective inhibitor[34] thio- and oxaflavopiridol (**3**) were identified as CDK1 selective inhibitors.[35] In addition, flavopiridol structure-based design led to the discovery of 2-benzylidene-

benzofuranone (**4**) as potent and selective inhibitor of CDK1[36] and recently P-276-00 (**5**) that was identified as a novel pan-selective CDK1 and -9 inhibitor.[37] Flavopiridol inhibits several kinases with IC₅₀ values 30-300 nM.[38] Actually, the advanced biology results created an increased demand for new small natural products derivatives [1] for drug discovery purposes. In order to emulate this approach, we found of great interest to explore new chemical space around the flavopiridol C ring with the purpose to identify unique structures with potential better cytotoxic activities. In this work, three series of flavopiridol analogues bearing various nucleus such as thiosugars (series 1), amino acids (series 2) as well as azoles moieties (series 3) tethered to the flavopiridol have been prepared (Figure 2). Their synthesis and *in vitro* cytotoxic antiproliferative activities as well as kinases inhibition are also presented.

2. Results and discussion

2.1. Chemistry

Although the chiral hydroxyl moiety on the D ring has been found to be essential for the anti CDK activity of flavopiridol, a recent study has demonstrated that replacing the chiral D ring with olefin analogue (tetrahydropyridyl) did not result in a major loss of CDK inhibitory activity.[34] However, from a synthetic point of view, we thought it is practical to pursue our present work with olefin moiety on the D ring since its synthesis could be achieved with less number of steps. Therefore, we have decided to focus our effort on exploring further modifications around the C ring in order to elaborate unique new structures and to examine their impact on the biological activity.

We first became interested to introduce thiosugars, the stable glycomimics of *O*-glycosides, with the intention to increase the solubility of the compounds and to improve their pharmacological properties and activities through the Warburg effects (Calvaresi, E. C.; Hergenrother, P. J. Glucose conjugation for the specific targeting and treatment of cancer *Chem Sci.* **2013**, *4*, 2319–2333). Then we envisioned the introduction of further groups like amino acids and azoles. These substituents will be introduced *via* a thioether (or amine) bonds on the *para*-iodo group of the 2-phenyl ring. (Figure 2).

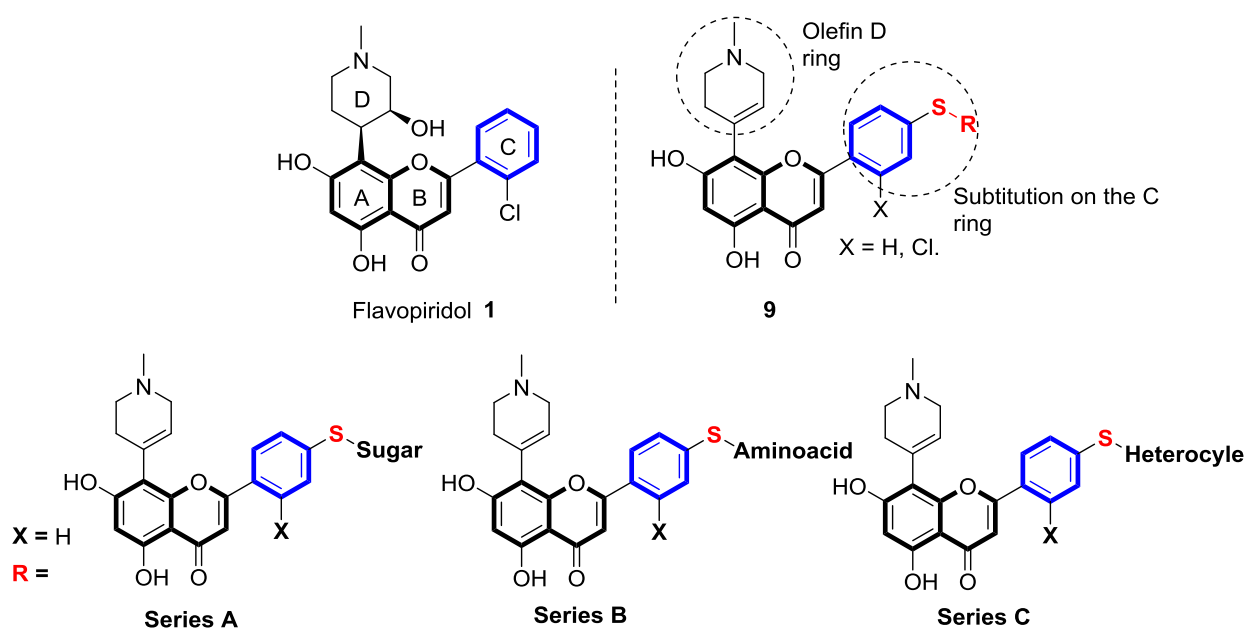
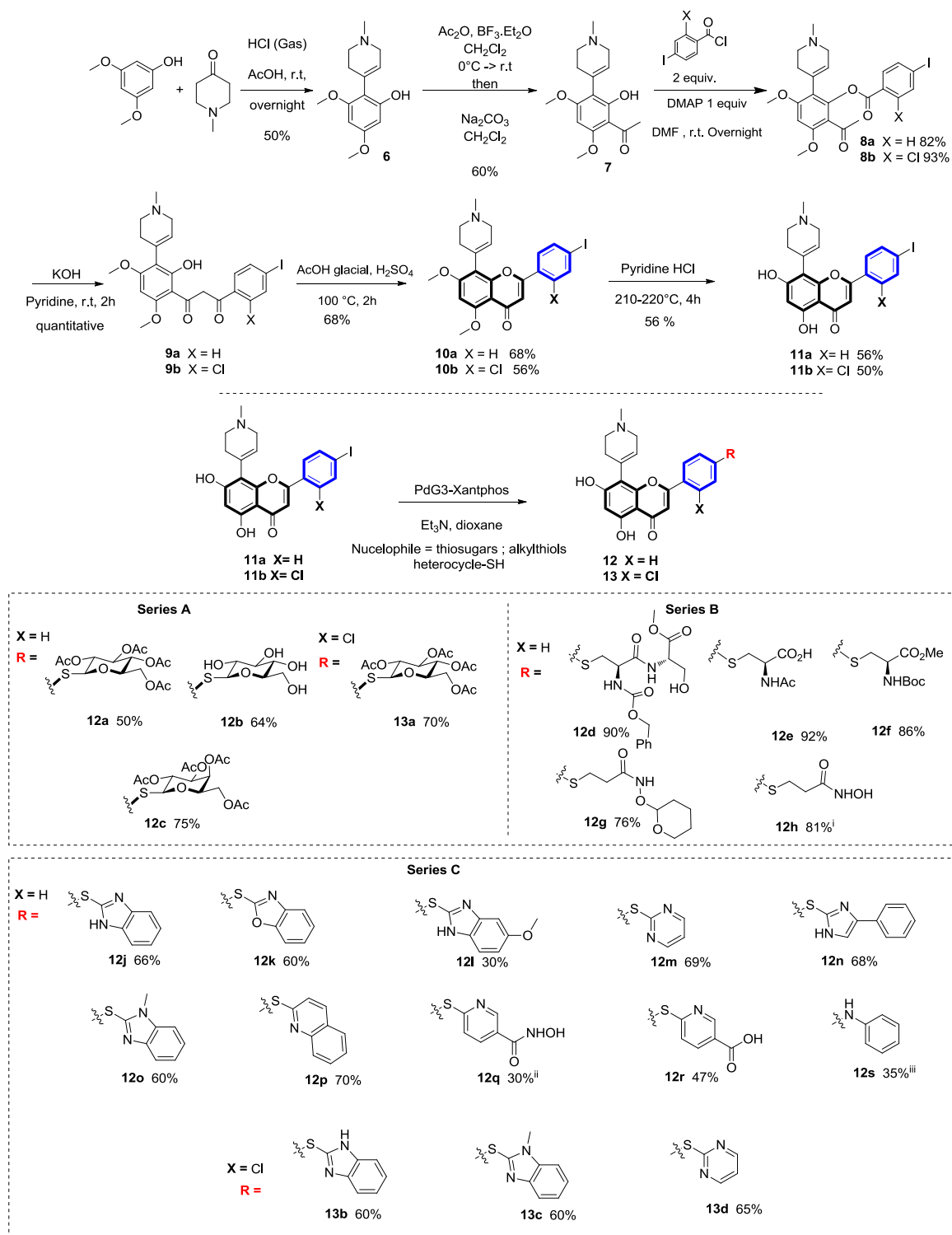


Figure 2. Flavopiridol-based structural approach for the conception of a new series presented in this study

Three different series of flavopiridol have been obtained in several step's synthetic pathways. First, the synthesis of flavopiridol analogues **11a-b** (Scheme 1) has been achieved over seven steps following a reproducible and robust previously reported method for a large-scale synthesis of flavopiridol.[39] Condensation of 3,5-dimethoxy phenol with

1-methyl-4-piperidinone in acetic acid saturated with anhydrous hydrogen chloride gas provided compound **6** in 50% yield. Friedel-Craft acylation of the aromatic compound **6** was accomplished by reaction with acetic anhydride and $\text{BF}_3\text{-OEt}_2$ followed by treatment of the resulting product under basic media in dichloromethane to afford **7** in 60 % yield. Benzoylation of compound **7** using 2-chloro-4-iodobenzoyl chloride 4-iodobenzoyl chloride generated the benzoate **8a**, and **8b** in 82% and 93% yields respectively. The Baker Venkataraman step has been then accomplished with powdered KOH in hot pyridine which smoothly isomerized the benzoate **8** to **9** in quantitative yield, this step was followed by the dehydration reaction which under catalytic sulfuric acid in acetic acid at 100°C allowed the formation of flavone **10a** and **10b** in 68 and 56 % yields respectively. The final step of the demethylation of the methyl ether-protecting groups was carried out under solvent-free conditions by heating a mixture of **10** and pyridine.HCl at 210 °C for 4 hours. Under these conditions, the final compound could be then obtained in 56% yield. We recently reported an efficient method allowing the introduction of glycosyl thiols to various iodo(hetero)aryles,[40] nucleic acids[41] and peptides ,[42] under simple and mild conditions using the palladium G3-Xanthphosbiphenyl precatalyst (Ref Chem Sci 2013 Buchwald et [ACS Catal. 2015, 5, 1386–1396](#)) . This method was adapted to our starting platform **11a-b**, furnishing the first two series (**a** and **b**) in which thiosugars and sulfur containing amino acids groups were tethered to the flavones core *via* a thioether bond.



Scheme 1. Synthetic route toward flavopiridol analogues. Substitution on the C ring with; Series A: thiosugars; Series B: aminoacids and alkyl chains; Series C: heterocycles. General conditions for the palladium catalyzed coupling reaction for products **13** and **14** formation: Pd-G3-Xantphos 5-10 mol%, Et₃N (3 equiv.), r.t. or 60°C, dioxane or dioxane/water. i: this compound was obtained from **13g** after cleavage of THP under acidic media. ii: yield calculated over two steps. iii: Cs₂CO₃ was used as base and the coupling was performed at 100 °C.

The thioglycoconjugation process could be performed rapidly and revealed to have a great tolerance towards functional groups (free OH and NH were well-tolerated). In order to develop a convergent synthetic strategy, the main challenge was to couple the unprotected iodo-flavopiridol **11** with the thiol-containing partners. Obviously, we were glad to observe again that precatalyst PdG3-Xantphos system was efficiently used for the first time with iodo-flavopiridol substrates (**11a** and **11b**) and protected β -thioglucose and β -galactose. Hence, with a catalytic amount of PdG3-Xantphos in a mixture of water and dioxane (see the experimental section for details) products (**12a**, **12c**, **13a**) were formed in good 50%, 75%, and 70 % yields respectively. The reaction was also successful with fully unprotected-thioglucose to generate compound **12b** in a 64 % yield. The same conditions were applied with sulfur-containing amino acids *N*-acetylcysteine, *N*-Boc-cysteine, and a dipeptide serine-cysteine as well as alkyl chain bearing hydroxamic acid moieties to give compound (**12d-h**) in up to 92 % yield. Thus, a third series (series **c**) of flavopiridol analogues has been built successfully as well with thiolated heterocycles. Products **12j-r** were obtained in up to 70 % yield and **13b-d** in up to 60 %. However, introducing amino heterocycles was more challenging and needed more heating (100°C), and the replacement of Et₃N with Cs₂CO₃ as a base source. Product issued from this coupling of **11a** with aniline was obtained in 35 % yield.

2.2. Biological results

2.2.1. In vitro antiproliferative activity

The antiproliferative effect of generated compounds has been assessed. The primary screening of series **A**, **B** and **C** was realized at one concentration of 10 μ M on ovarian cancer cell line (SKOV3). Note here that 100% of cell viability was obtained for DMSO-treated cells. All compounds issued from series **A** and **B** did not show a growth inhibition superior to 50 %, while compounds from series **C** showed more interesting activities. Therefore, the IC₅₀ values were determined for series **C** compounds on the SKOV3 cell line (Table 1). In series **A**, compounds having a sugar unit were found ineffective (**12a** and **12b**) or with moderate activity (compounds **12c** and **13a**). Derivatives containing amino acid moieties (Series **B**) also gave low to moderate cytotoxic activity (compounds **12d-h**). Compounds issued from Series **C** having heterocyclic substituents, in particular, benzimidazole and imidazole ring were found to be the more active compounds, and they gave on IC₅₀ in the sub-micromolar range (compounds **12j**, **12n**, **12o**, **13b**, **13c**).

Table 1.

Cell-based primary screening for selection of compounds with antiproliferative activity.

compd	12a	12b	12c	12d	12e	12f	12g
IC ₅₀ (μ M) ^a	Na ^b	Na ^b	2.87 \pm 1.9	4.3 \pm 0.03	Na ^b	7.79 \pm 1.6	6.85 \pm 2.7
SKOV3							
compd	12h	12j	12k	12l	12m	12n	12o
IC ₅₀ (μ M) ^a	Na ^b	0.59 \pm 0.07	2.0 \pm 1.2	1.2 \pm 0.5	Na ^b	0.29 \pm 0.08	0.34 \pm 0.013
compd	12p	12q	12r	12t	13a	13b	13c
IC ₅₀ (μ M) ^a	3.8 \pm 1.2	Na ^b	Na ^b	1.2 \pm 0.5	2.33 \pm 1.6	0.33 \pm 0.07	0.09 \pm 0.045
compd	13d	flavopiridol					
IC ₅₀ (μ M) ^a	Na ^b	0.22 \pm 0.06					

^a IC₅₀ values are reported in μ M. The IC₅₀ is the concentration of compound required to decrease cell growth by 50%; values represent the means \pm SD of three experiments.

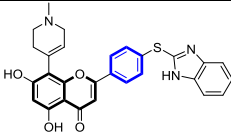
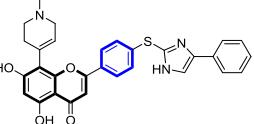
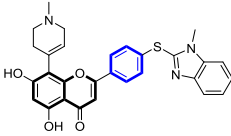
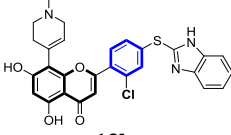
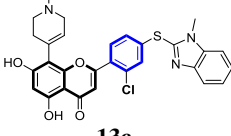
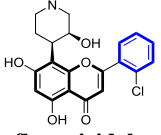
^b Na: not active, (IC₅₀ > 10 μ M).

After this first screening of generated compounds on SKOV3, the five most active compounds were selected for evaluation against six additional human cancer cell lines and compared with the reference compound, the flavopiridol (Table 2).

Except compound **12n** having imidazole group, all the other selected compounds were found active on the six tested cell lines with IC₅₀ values less than 1 μM. Overall, the presence of benzimidazole moieties seem to be important for the cytotoxic effect of these compounds. *N*-methyl benzimidazole derivatives showed more cytotoxic activity in comparison to their no methylated counterpart (compound **12j** vs **12o**). Finally, the presence of chlorine atom on the phenyl group tethered to chromenone ring display better activity, in comparison to the free-chlorine compounds (compound **13b** vs **12j**, and compound **12o** vs **13c**). This SAR led us to identify **13c** as the most active compound, with an IC₅₀ < 100 nM on 6 cancer cell lines, and it was found more cytotoxic than the reference compound, the flavopiridol.

Table 2.

Antiproliferative activities of selected compounds against a panel of seven human cancer cell lines, IC₅₀ values are reported in nM.

Compound	SKOV3 ^a	NCI-N87 ^b	SKBR3 ^c	PC3 ^d	MiaPaCa-2 ^e	HCT116 ^f	K562 ^g
 12j	595 ± 73	183 ± 81	253.8 ± 162	742 ± 21	852 ± 59	293 ± 7	194 ± 11
 12n	295 ± 88	4796 ± 1271	352 ± 37	243 ± 88	448 ± 80	173 ± 18	300 ± 59
 12o	344 ± 13	391 ± 86	249 ± 22.9	276 ± 64	361 ± 18	219 ± 18	345 ± 4.9
 13b	333 ± 72	12 ± 1.1	66.6 ± 2.5	326 ± 10	361 ± 18	170 ± 2	36 ± 4
 13c	94 ± 45	49 ± 2	53.7 ± 4.1	85 ± 9.5	52.9 ± 6.8	81 ± 23	50.8 ± 2.8
 flavopiridol	220 ± 60	111 ± 10.2	75 ± 3.2	110 ± 5	320 ± 21.5	20 ± 2.5	125 ± 24.2

^a SKOV3, ovarian cancer cells; ^b NCI-N87, gastric adenocarcinoma cells; ^c SKBR3, breast cancer cells; ^d PC3, prostate cancer cells; ^e MiaPaCa-2, pancreatic cancer cells; ^f HCT116, colon-carcinoma cells; ^g K562, immortalised myelogenous leukemia cell line.

2.2.2. Kinase enzymatic assays.

In order to study the mechanism of action of the more active compounds, we tested their effect on the inhibition of the enzymatic activities of protein kinases as putative targets. A panel of eight serine/threonine protein kinases was tested including cyclin-dependent kinases (*HsCDK2/cyclin A*, *HsCDK5/p25*, *HsCDK9/cyclinT*), glycogen synthase kinase-3 beta (*HsGSK3β* and *SscGSK-3α/β*), porcine casein kinase 1 (*SscCK1δ/ε*), *Leishmania major* casein kinase 1 (*LmCK1*), and *Plasmodium falciparum* glycogen synthase kinase-3 (*PfGSK3*). The percentage of residual

activity at 10 μ M and 1 μ M were used to characterize the bioactivity of the compounds during the primary screening campaign (Table 3).

Table 3.
Kinase-based primary screening.^a

compd	CC	<i>Hs</i> -CDK2/ CyclinA	<i>Hs</i> -CDK5/ p25	<i>Hs</i> -CDK9/ CyclinT	<i>Hs</i> -GSK3 β	<i>Lm</i> -CK1	<i>Pf</i> -GSK3	<i>Ssc</i> - CK1 δ/ϵ	<i>Ssc</i> - GSK3 α/β
Flavopiridol	10 μ M	11	13	1	10	61	70	78	16
	1 μ M	26	36	5	50	≥ 100	≥ 100	≥ 100	70
13b	10 μ M	22	14	3	4	35	64	48	4
	1 μ M	46	42	2	14	81	≥ 100	86	43
12n	10 μ M	14	5	0	6	54	≥ 100	43	11
	1 μ M	33	10	2	25	88	≥ 100	78	53
12o	10 μ M	25	26	-4	-3	57	79	41	8
	1 μ M	51	41	-2	31	68	80	83	41
13c	10 μ M	30	24	-2	2	38	46	62	10
	1 μ M	87	68	1	12	62	80	90	31
12j	10 μ M	5	4	10	-8	40	54	69	11
	1 μ M	35	14	8	6	99	85	91	36

^a Kinase activities in the presence of 10 or 1 μ M of tested compounds were measured by ADP-Glo luminescent assay (Promega, Madison, WI, USA), using 10 μ M ATP. Data are mean (n = 2) expressed in % of maximal activity, compared with a DMSO control. The red color scale is used to highlight the values that are below 50% of residual kinase activity. (% of residual activity at 10 μ M and 1 μ M). ≥ 100 indicates that the compound cannot inhibit the enzymatic activity at the tested concentration. CC, concentration tested.

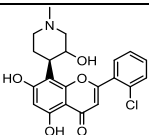
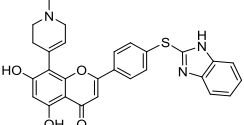
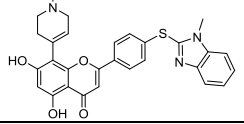
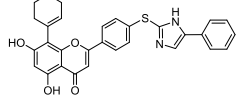
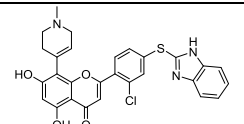
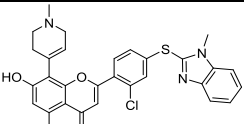
Overall, all tested compounds were found to inhibit slightly the activity of no human kinases, *Lm*-CK1, *Pf*-GSK3, and *Ssc*-CK1 δ/ϵ kinases (only at high dose 10 μ M). At low dose (1 μ M), moderate to good activity was observed for *Hs*-CDK2/CyclinA, *Hs*-CDK5/p25, *Hs*-CDK9/CyclinT, *Hs*-GSK3 β , and *Ssc*-GSK3 α/β kinases.

Compounds displaying more than 70% inhibition at 10 μ M were next tested over a wide range of concentrations (usually from 0.0003 to 10 μ M) on human kinases and IC₅₀ values were determined from the dose response curves (Prism-GraphPad, GraphPad Software, San Diego, CA, USA). The results of the *in vitro* kinase assay were summarized in Table 4.

The cyclin-dependent kinases (CDKs), a subfamily of serine-threonine kinases, play an important role in the cell cycle regulation. Inhibition of cell cycle CDKs has been proven an efficient anticancer strategy. Concerning the inhibition of CDK2 and CDK5, the presence of a chlorine atom on the phenyl ring (compounds **13b** and **13c**) led to a decrease of the activity in comparison to the reference compound, the flavopiridol. However, no-chlorinated compounds (**12j**), (**12o**), and even imidazole derivative (**12n**) showed an interesting inhibition of these two kinases, similar to flavopiridol. Thus, compound **12j** displayed the best activity with an IC₅₀ of 0.162 and 0.121 μ M which is better than the reference compound. Cyclin-dependent protein kinase 9 (CDK9) has been shown to play an important role in the pathogenesis of malignant tumors.[43] CDK9 inhibitors have demonstrated antitumoral activity *in vitro*. All the tested compounds in

this study exhibited high inhibition toward this kinase with an IC_{50} similar or better than the flavopiridol. Interestingly, compounds **12j** and **12n** displayed an IC_{50} in the nM range.

Table 4.
 IC_{50} values and structures of flavopiridol analogues (IC_{50} in μM)^a

Compound	<i>HsCDK2/CyclinA</i>	<i>HsCDK5/p25</i>	<i>HsCDK9/CyclinT</i>	<i>HsGSK3β</i>
Flavopiridol 	0.379	0.272	0.011	1.184
12j 	0.162	0.121	0.008	0.117
12o 	0.349	0.284	0.014	0.160
12n 	0.469	0.195	0.009	0.356
13b 	1.556	0.550	0.015	0.216
13c 	1.725	1.093	0.064	0.059

a. IC_{50} values are reported in μM . IC_{50} values. Activities were assessed in duplicate using the ADP-Glo luminescent assay (Promega), using 10 μM ATP.

b. Kinases activities were assayed in duplicate.

GSK-3 is a ubiquitously expressed serine/threonine kinase, it is involved in many signaling pathways controlling many different key functions. Numerous studies show that GSK3 action supports cancer cells and suggest that its inhibition may have therapeutic benefits. The GSK-3 activity has been linked to many pathogenesis including colorectal cancer, diabetes, acute myeloid leukemia and Alzheimer's disease.[44] The biological assay showed that all the tested compounds inhibit more efficiently human isoform β of GSK3 in comparison to the flavopiridol. Compound **13c** displayed the best activity with an IC_{50} of 59 nM, which is 20 folds more active than flavopiridol.

Taken together, these results showed that compounds **12j** and **12n** which showed a moderate or low cytotoxic activity respectively, inhibit efficiently the activity of CDK9 kinase. Importantly, compound **13c** which have the best cytotoxic activity displays a very good selectivity towards CDK9 and GSK3 β kinases in comparison to CDK2 and 5, offering new potential targets for this compound.

Following the characterization of the kinases as putative targets driving the cytotoxicity phenotype, we then decided to explore the putative binding mode of the more active compound on the more affected target. We thus decided to select compound **13c** and human GSK3 β . The remaining % of maximal activity (compared with a DMSO control) were determined at ATP concentrations of 3.125, 6.25, 12.5, 25, 50 and 100 μ M. As shown on figure 3, the results obtained strongly suggest an ATP-competitive inhibition of GSK3 β by **13c**. The inhibition of the kinase activity is almost fully abrogated by the highest tested concentration of ATP (100 μ M). Note here that this ATP competitive binding mode was also reported for the inhibition of CDKs by flavopiridol.[8]

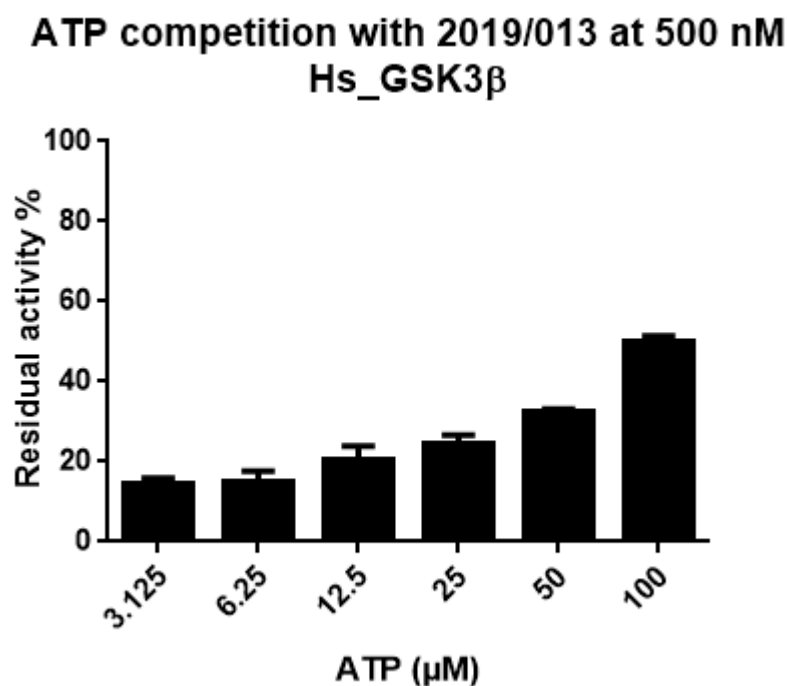


Fig. 3. Human GSK-3 β inhibition by compound **13c** at different ATP concentrations. GSK-3 β kinase activities in the presence of 500 nM of **13c** were measured by ADP-Glo luminescent assay using the mentioned ATP concentrations (from 3.125 to 100 μ M). Data are mean ($n = 3$) \pm SD expressed in % of residual activity, compared with a DMSO control.

Conclusion

We have shown successfully a convergent route to synthesize flavopiridol analogs modified at the C ring by means of PdG3-Xanthphos precatalyst. The cross-coupling was realized directly between no protected iodo-flavopiridol and thiol sugars, amino acids, and heterocycles under mild conditions. The synthesis allowed us to access three series of new and unique structures. Cytotoxic activities of benzimidazoles containing flavopiridol presented in this work are comparable and even higher than flavopiridol. We showed also that the enzymatic activity of some of the tested kinase, including GSK3 β , are potently affected by selected molecular hits. Among all tested compounds, compound **13c** showed the best antiproliferative activity associated with an inhibition of CDK9, and GSK3 β in the nM range. These results constitute a

starting point enabling a better understanding of structure-activity relationships of this new series of compounds and should facilitate future elaboration to more efficient and selective inhibitors of CDK9 and GSK3 β which may have applications in affecting the pathogenesis of cancer and Alzheimer's disease. Dual- or multi-target kinase inhibitors for developing new polypharmacological approaches can also be explored using these new flavopiridol derivatives.

4. Experimental

4.1. Materials

Solvents and reagents are obtained from commercial suppliers and were used without further purification. Analytical TLC was performed using Merck silica gel F254 (230-400 mesh) plates and analyzed by UV light or by staining upon heating with vanillin solution. For silica gel chromatography, the flash chromatography technique was used, with Merck silica gel 60 (230-400 mesh) and p.a. grade solvents unless otherwise noted. The ^1H NMR and ^{13}C NMR spectra were recorded in either CDCl_3 , MeOD, or DMSO-*d*6 on Bruker Avance 300 or 400 spectrometers. The chemical shifts of ^1H and ^{13}C are reported in ppm relative to the solvent residual peaks. IR spectra were measured on a Perkin Elmer spectrophotometer. High resolution mass spectra (HR-MS) were recorded on a MicroMass LCT Premier Spectrometer. Thiosugars were synthesized as according the following protocols.[45, 46] The Xantphos palladium precatalyst third generation was synthesized according to literature protocol.[47] **6** and Acetophenone **7** was prepared adopting reported methods spectral data are in agreement with the published ones.[48]

4.2. Chemistry

4.2.1. Synthesis of the intermediates

4.2.1.1. *2-acetyl-3,5-dimethoxy-6-(1-methyl-1,2,3,6-tetrahydropyridin-4-yl)phenyl 4-iodobenzoate (8a)*. A mixture of **7** (1.0 g, 0.0034 moles), 4-iododbenzoic acid chloride (1.8 g, 0.0068 moles) and DMAP (0.414 g, 0.0034 moles) was stirred overnight in DMF (40 mL) at r.t. After DMF was removed, the residue was dissolved in DCM and washed with saturated solution of bicarbonate, the organic layer was dried over MgSO_4 . The crude residue was purified by flash chromatography (DCM/MeOH 0 \rightarrow 3 %). The product was obtained as orange solid in 82% yield. ^1H NMR (300 MHz, CDCl_3) δ 7.81 (q, J = 8.7 Hz, 4H), 6.42 (s, 1H), 5.55 (s, 1H), 3.92 (s, 3H), 3.86 (s, 3H), 2.94 (s, 2H), 2.58 (s, 2H), 2.47 (s, 3H), 2.33 (s, 2H). HR-ESIMS: m/z 522.0797 [$\text{M} + \text{H}$] $^+$ (calcd for $\text{C}_{23}\text{H}_{25}\text{INO}_5$, 522.0778).

4.2.1.2. *2-acetyl-3,5-dimethoxy-6-(1-methyl-1,2,3,6-tetrahydropyridin-4-yl)phenyl 2-chloro-4-iodobenzoate (8b)*. A mixture of **7** (0.800 g, 0.0027 moles), 3-chloro,4-iododbenzoic acid chloride (1.400 g, 0.0046 moles) and DMAP (0.441 g, 0.0036 moles) was stirred overnight in DMF (30 mL) at r.t. After DMF was removed, the residue was dissolved in DCM and washed with saturated solution of bicarbonate, the organic layer was dried over MgSO_4 . The crude residue was purified by flash chromatography (DCM/MeOH 0 \rightarrow 3%). The product was obtained as orange solid in 93% yield. ^1H NMR (300 MHz, CDCl_3) δ 7.88 (s, 1H), 7.72 (s, 2H), 6.43 (s, 1H), 5.64 – 5.54 (m, 1H), 3.93 (s, 3H), 3.88 (s, 3H), 2.96 (s, 2H), 2.53 (m, 5H), 2.34 (m, 5H). ^{13}C NMR (75 MHz, CDCl_3) δ 159.94, 158.05, 139.44, 136.01, 134.89, 132.97, 128.66, 125.89, 116.71, 104.44, 99.01, 93.15, 55.89, 54.53, 52.18, 45.76, 32.04, 30.92, 29.31.

4.2.1.3. *2-(4-iodophenyl)-5,7-dimethoxy-8-(1-methyl-1,2,3,6-tetrahydropyridin-4-yl)-4H-chromen-4-one (10a)*. According to the protocol of Tabaka et al.[39] A round-bottom flask equipped with an overhead stirrer was charged with **8a** (1 g, 0.0019 moles) and pyridine (6 mL) and heated to 55 $^\circ\text{C}$. Freshly pulverized KOH (158 mg, 2.82 mmol) was added with stirring and the heating continued for 3 hours. The resulting black mixture was poured into a mixture of H_2O and HCl (concentrated) and allowed to stand for 30 min. While the mixture cooled, the pH was adjusted to 9 with Na_2CO_3 (saturated), and the aqueous layer was extracted with 5% MeOH in CHCl_3 . The combined organic layers were washed with H_2O and brine, dried (MgSO_4), filtered and concentrated under reduced pressure. The crude Compound **9** was used as it is in the next step of synthesis. A round-bottom flask was charged with **9** (1 g, 0.0019 moles), AcOH (20 mL), and H_2SO_4 (concentrated, 2.2 mL) and heated to 100 $^\circ\text{C}$. Heating was maintained for 2 h followed by cooling to rt overnight. The reaction was concentrated on a rotary evaporator, diluted with H_2O , and neutralized by the addition of Na_2CO_3 (saturated) to pH 9. The aqueous layer was extracted with 5% MeOH in CHCl_3 . The combined organics were dried (MgSO_4), filtered, and concentrated under reduced pressure. The product was purified by chromatography, DCM-MeOH (2 \rightarrow 4 %) to yield **10a** as a yellow solid (68%). ^1H NMR (300 MHz, CDCl_3) δ 7.85 (d, J = 8.5 Hz, 2H), 7.59 (d, J = 8.6 Hz, 2H), 6.66 (s, 1H), 6.44 (s, 1H), 5.72 (s, 1H), 4.03 (s, 3H), 3.93 (s, 3H), 3.20 (m, 2H), 2.74 (m, 2H), 2.48 (m, 5H). ^{13}C NMR (75 MHz, CDCl_3) δ 177.94, 161.02, 160.04, 155.30, 138.20, 131.27, 128.03, 127.37, 126.54, 108.70, 108.16, 97.84, 91.69, 56.45, 55.91, 54.96, 52.60, 46.02, 29.90, 1.02. HR-ESIMS: m/z 504.0670 [$\text{M} + \text{H}$] $^+$ (calcd for $\text{C}_{23}\text{H}_{23}\text{INO}_4$, 504.0672).

4.2.1.4. 2-(2-chloro-4-iodophenyl)-5,7-dimethoxy-8-(1-methyl-1,2,3,6-tetrahydropyridin-4-yl)-4H-chromen-4-one (**10b**). According to the protocol of Tabaka et al.[39] A round-bottom flask equipped with an overhead stirrer was charged with **8a** (1 g, 0.0019 moles) and pyridine (6 mL) and heated to 55 °C. Freshly pulverized KOH (158 mg, 2.82 mmol) was added with stirring and the heating continued for 3 hours. The resulting black mixture was poured into a mixture of H₂O and HCl (concentrated) and allowed to stand for 30 min. While the mixture cooled, the pH was adjusted to 9 with Na₂CO₃ (saturated), and the aqueous layer was extracted with 5% MeOH in CHCl₃. The combined organic layers were washed with H₂O and brine, dried (MgSO₄), filtered and concentrated under reduced pressure. The crude Compound **9b** was used as it is in the next step of synthesis. A round-bottom flask was charged with **9** (280 mg, 0.5 mmol), AcOH (5.5 mL), and H₂SO₄ (concentrated, 0.6 mL) and heated to 100 °C. Heating was maintained for 2 h followed by cooling to rt overnight. The reaction was concentrated on a rotary evaporator, diluted with H₂O, and neutralized by the addition of Na₂CO₃ (saturated) to pH 9. The aqueous layer was extracted with 5% MeOH in CHCl₃. The combined organics were dried (MgSO₄), filtered, and concentrated under reduced pressure. The product was purified by chromatography, DCM-MeOH (2 → 4 %) to yield **10b** as a yellow solid (56%). ¹H NMR (300 MHz, CDCl₃) δ 7.89 (d, *J* = 1.5 Hz, 1H), 7.73 (dd, *J* = 8.2, 1.5 Hz, 1H), 7.35 (d, *J* = 8.2 Hz, 1H), 6.60 (s, 1H), 6.45 (s, 1H), 5.65 (s, 1H), 4.03 (s, 3H), 3.93 (s, 3H), 3.13 (d, *J* = 2.6 Hz, 2H), 2.67 (t, *J* = 5.5 Hz, 2H), 2.42 (m, 5H).

4.2.1.5. 5,7-dihydroxy-2-(4-iodophenyl)-8-(1-methyl-1,2,3,6-tetrahydropyridin-4-yl)-4H-chromen-4-one (**11a**). A round-bottom flask was charged with **10a** (500 mg, 0.99 mmol) and pyridine hydrochloride (1.138 g, 9.9 mmol) and heated in an oil bath to 210-220 °C for 4 h. The mixture was neutralized and extracted with 5% MeOH in CHCl₃. The crude residue was purified by flash chromatography (DCM/MeOH 5 → 10 %). Yellow solid 56%. ¹H NMR (300 MHz, DMSO) δ 12.83 (s, 1H), 8.21 (s, 1H), 7.97 (d, *J* = 8.2 Hz, 2H), 7.76 (d, *J* = 8.3 Hz, 2H), 7.01 (s, 1H), 6.32 (s, 1H), 5.72 (s, 1H), 3.17 (s, 2H), 2.71 (s, 2H), 2.41 (s, 5H). ¹³C NMR (75 MHz, DMSO) δ 159.97, 138.51, 128.38, 126.60, 109.97, 109.28, 105.96, 105.25, 98.73, 54.24, 51.78, 45.52, 34.20, 29.27. HR-ESIMS: *m/z* 476.0356 [M + H]⁺ (calcd for C₂₁H₁₉INO₄, 476.0359).

4.2.1.6. 2-(2-chloro-4-iodophenyl)-5,7-dihydroxy-8-(1-methyl-1,2,3,6-tetrahydropyridin-4-yl)-4H-chromen-4-one (**11b**). A round-bottom flask was charged with **10b** (500 mg, 0.99 mmol) and pyridine hydrochloride (1.138 g, 9.9 mmol) and heated in an oil bath to 210-220 °C for 4 h. The mixture was neutralized and extracted with 5% MeOH in CHCl₃. The crude residue was purified by flash chromatography (DCM/MeOH 5 → 10%). Yellow solid 50%. ¹H NMR (300 MHz, MeOD) δ 8.05 (s, 1H), 7.91 (d, *J* = 7.9 Hz, 1H), 7.43 (d, *J* = 8.3 Hz, 1H), 6.53 (s, 1H), 6.36 (s, 1H), 5.81 (s, 1H), 2.98 (s, 2H), the other signals are overlapped with solvent.

4.2.2. General procedure for the synthesis of compounds **12** and **13**:

Coupling of **11a** and **11b** with thiol partners or with aniline:

A sealable tube purged with argon equipped with a cap was charged with **11a** or **11b** (1 equiv), thiosugars, thioheterocycles or aniline (1 to 1.5 equiv), PdG3-Xantphos (a mettre une ref pour dire que le PDG3 est synthétisé selon le ChemSci 2013 de Buchwald car nous n'avons pas utilisé du commercial) (5 to 10 mol%), the tube was flushed again with Argon, then degassed dioxane (and water when mentioned), and Et₃N or Cs₂CO₃ (1 to 6 equiv) were added. The mixture was stirred at r.t. or 60 °C or at 100 °C for the corresponding times (see details time below). Purification was performed with flash chromatography on silica gel using a gradient of methanol in dichloromethane or by preparative HPLC using a gradient of acetonitrile in water.

4.2.2.1. (3*R*,4*S*,5*S*,6*S*)-2-(acetoxymethyl)-6-((4-(5,7-dihydroxy-8-(1-methyl-1,2,3,6-tetrahydropyridin-4-yl)-4-oxo-4H-chromen-2-yl)phenyl)thio)tetrahydro-2H-pyran-3,4,5-triyl triacetate (**12a**). **11a** (20 mg, 0.04 mmol), β-thiosugar (17 mg, 0.042 mmol), PdG3-Xantphos (5 mol%), Et₃N (10 μL) and dioxane (1 mL) were stirred at r.t. for 2 hours. The compound was purified over silica gel (DCM/MeOH, 5 → 7%) and obtained as yellow solid in 50% yield. ¹H NMR (300 MHz, DMSO) δ 12.88 (s, 1H), 7.97 (d, *J* = 8.4 Hz, 2H), 7.60 (d, *J* = 8.4 Hz, 2H), 7.02 (s, 1H), 6.33 (s, 1H), 5.73 (s, 1H), 5.55 (d, *J* = 10.1 Hz, 1H), 5.42 (t, *J* = 9.4 Hz, 1H), 4.95 (q, *J* = 9.5 Hz, 2H), 4.15 (dt, *J* = 23.9, 9.0 Hz, 3H), 3.19 (m br, 2H), 2.73 (m br, 2H), 2.43 (s, 6H), 1.96 (m, 12H). ¹³C NMR (75 MHz, DMSO) δ 182.68, 170.41, 169.96, 169.75, 169.54, 162.77, 162.22, 160.24, 154.28, 138.27, 130.24, 129.95, 127.64, 127.19, 126.49, 109.98, 109.34, 105.16, 104.26, 99.14, 82.69, 74.83, 73.31, 69.90, 68.51, 62.35, 54.53, 52.10, 45.48, 29.46, 29.21, 20.99, 20.84, 20.73; *v*_{max} 2987, 2901, 1747, 1651, 1579, 1405, 1372, 1223, 1042, 909, 825, 563, 488 cm⁻¹; HR-ESIMS: *m/z* 712.2058 [M + H]⁺ (calcd for C₃₅H₃₈NO₁₃S, 712.2064). HPLC purity, 98.5% (*t*_R = 11.22 min).

4.2.2.2. 5,7-dihydroxy-8-(1-methyl-1,2,3,6-tetrahydropyridin-4-yl)-2-(4-(((2*S*,3*S*,4*S*,5*S*)-3,4,5-trihydroxy-6-(hydroxymethyl)tetrahydro-2H-pyran-2-yl)thio)phenyl)-4H-chromen-4-one (**12b**). **11a** (30 mg, 0.063 mmol), β-thiosugar (18 mg, 0.091 mmol), PdG3-Xantphos (8 mol%), Et₃N (60 μL), water (0.2 mL) and dioxane (1 mL) were stirred at 60 °C for 2 hours. The compound was purified with over silica gel (DCM/MeOH, 5 → 15 %) and obtained as yellow solid in 64% yield. ¹H NMR (300 MHz, MeOD) δ 8.45 (s, 1H), 7.82 (d, *J* = 7.9 Hz, 2H), 7.68 (d, *J* = 7.7 Hz,

2H), 6.68 (s, 1H), 6.29 (s, 1H), 5.85 (s, 1H), 4.81 (signal overlapped with water), 3.97-3.93 (m, 3H), 3.73-3.68 (m, 1H), 3.52-3.48 (m, 4H), 3.38-3.31 (m, 5H overlapped with MeOD), 3.02 (s, 3H), 2.81 (s, 2H). ¹³C NMR (75 MHz, MeOD) δ 182.53, 163.66, 161.94, 161.11, 154.28, 140.72, 129.49, 128.85, 128.74, 126.36, 121.47, 109.99, 106.93, 104.23, 98.53, 86.76, 80.93, 78.35, 72.49, 70.04, 61.60, 51.97, 50.61, 41.68, 25.78; ν_{\max} 2987, 2900, 1650, 1560, 1408, 1374, 1273, 1187, 1056, 825, 770, 745, 550 cm⁻¹; HR-ESIMS: m/z 544.1649 [M + H]⁺ (calcd for C₂₇H₃₀NO₉S⁺, 544.1641). HPLC purity, >90% (t_R = 8.24 min).

4.2.2.3. (3*S*,4*S*,5*S*,6*S*)-2-(acetoxymethyl)-6-((4-(5,7-dihydroxy-8-(1-methyl-1,2,3,6-tetrahydropyridin-4-yl)-4-oxo-4*H*-chromen-2-yl)phenyl)thio)tetrahydro-2*H*-pyran-3,4,5-triyl triacetate (**12c**). **11a** (20 mg, 0.04 mmol), β -thiosugar (17 mg, 0.042 mmol), PdG3-Xantphos (5 mol%), Et₃N (50 μ L), and dioxane (1 mL) were stirred at r.t. for 2 hours. The compound was purified with over silica gel (DCM/MeOH, 0 \rightarrow 5%) and obtained as beige solid in 75 % yield. ¹H NMR (300 MHz, CDCl₃) δ 12.68 (s, 1H), 7.71 (d, J = 18.9 Hz, 4H), 6.61 (s, 1H), 5.90 (s, 1H), 5.49 (s, 1H), 5.31 (t, J = 10.0 Hz, 1H), 5.15 (d, J = 9.4 Hz, 1H), 4.98 (d, J = 9.5 Hz, 1H), 4.28-4.15 (m, 4H), 3.74 (s, 2H), 3.39 (s, 2H), 2.89 (s, 5H), 2.08 (m, 12 H). ¹³C NMR (75 MHz, CDCl₃) δ 182.22, 170.47, 170.12, 169.98, 169.59, 162.91, 161.39, 160.98, 154.24, 138.33, 131.07, 129.93, 129.09, 126.53, 124.07, 106.75, 105.61, 104.96, 99.72, 85.18, 77.46, 77.03, 76.61, 74.45, 71.82, 67.11, 61.28, 53.04, 51.59, 43.88, 27.49, 20.86, 20.70, 20.59; ν_{\max} 2971, 2900, 1743, 1648, 1561, 1489, 1407, 1369, 1241, 1065, 825, 559 cm⁻¹; HR-ESIMS: m/z 712.2076 [M + H]⁺ (calcd for C₃₅H₃₈NO₁₃S⁺, 712.2064); HPLC purity, 94.09 % (t_R = 11.80 min).

4.2.2.4. (3*R*,4*S*,5*S*,6*S*)-2-(acetoxymethyl)-6-((3-chloro-4-(5,7-dihydroxy-8-(1-methyl-1,2,3,6-tetrahydropyridin-4-yl)-4-oxo-4*H*-chromen-2-yl)phenyl)thio)tetrahydro-2*H*-pyran-3,4,5-triyl triacetate (**13a**). **11b** (50 mg, 0.098 mmol), β -thiosugar (40 mg, 0.11 mmol), PdG3-Xantphos (10 mol%), Et₃N (100 μ L), and dioxane (2 mL) were stirred at 60°C for 2 hours. The compound was purified with over silica gel (DCM/MeOH, 0 \rightarrow 5 %) and obtained as yellow solid in 70% yield. ¹H NMR (300 MHz, MeOD) δ 7.73 (s, 1H), 7.62 (dd, J = 22.0, 8.0 Hz, 2H), 6.52 (s, 1H), 6.31 (s, 1H), 5.78 (s, 1H), 5.38 (t, J = 9.3 Hz, 1H), 5.22 (d, J = 10.0 Hz, 1H), 5.13 – 4.93 (m, overlapped with solvent 5H), 4.36 – 4.17 (m, 2H), 4.07 (s, 1H), 3.59 (s, 2H), 3.18 (s, 2H), 2.74 (s, 3H), 2.64 (s, 2H), 2.05 (dd, J = 22.9, 10.0 Hz, 12H). ¹³C NMR (75 MHz, MeOD) δ 182.11, 170.81, 170.03, 169.79, 169.54, 154.88, 138.05, 132.40, 132.14, 130.90, 130.39, 129.74, 128.20, 123.27, 110.29, 99.05, 83.51, 75.44, 73.69, 69.66, 68.07, 61.85, 52.76, 50.98, 42.53, 26.99, 19.40, 19.22, 19.13; HR-ESIMS: m/z 746.1682 [M + H]⁺ (calcd for C₃₅H₃₇NO₁₃SCl, 746.1674); HPLC purity, 94% (t_R = 11.66 min).

4.2.2.5. (*S*)-methyl 2-((*R*)-2-(((benzyloxy)carbonyl)amino)-3-((4-(5,7-dihydroxy-8-(1-methyl-1,2,3,6-tetrahydropyridin-4-yl)-4-oxo-4*H*-chromen-2-yl)phenyl)thio)propanamido)-3-hydroxypropanoate (**12d**). **11a** (30 mg, 0.063 mmol), thio-dipeptide (27 mg, 0.075 mmol), PdG3-Xantphos (8 mol%), Et₃N (60 μ L), and dioxane (1.5 mL) were stirred at r.t. for overnight. The compound was purified with over silica gel (DCM/MeOH, 0 \rightarrow 7 %) and obtained as orange solid in 90% yield. ¹H NMR (300 MHz, MeOD) δ 7.78 (d, J = 7.6 Hz, 2H), 7.51 (s, 2H), 7.40 – 7.21 (m, 5H), 6.62 (s, 1H), 6.24 (s, 1H), 5.75 (s, 1H), 5.09 (s, 2H), 4.75 (s, 1H), 4.25 (s, 1H), 3.79 (d, J = 4.2 Hz, 2H), 3.71 (s, 3H), 3.58 (m, 4H), 3.14 (s, 2H), 2.73 (s, 3H), 2.62 (s, 2H). ¹³C NMR (75 MHz, MeOD) δ 182.39, 179.96, 178.43, 171.43, 170.46, 163.23, 160.71, 156.92, 154.24, 140.98, 128.47, 128.08, 127.63, 127.42, 126.51, 123.88, 108.09, 103.93, 103.70, 99.03, 66.43, 61.83, 56.83, 53.17, 52.11, 51.78, 51.32, 43.19, 33.51, 29.38, 27.42; ν_{\max} 1648, 1561, 1405, 1370, 1241, 1065, 826, 741, 698, 560 cm⁻¹; HR-ESIMS: m/z 704.2283 [M + H]⁺ (calcd for C₃₆H₃₈N₃O₁₀S, 704.2278); HPLC purity, 92% (t_R = 10.68 min).

4.2.2.6. *N*-acetyl-*S*-(4-(5,7-dihydroxy-8-(1-methyl-1,2,3,6-tetrahydropyridin-4-yl)-4-oxo-4*H*-chromen-2-yl)phenyl)-*D*-cysteine (**12e**). **11a** (30 mg, 0.063 mmol), *N*-acetylcysteine (14 mg, 0.08 mmol), PdG3-Xantphos (8 mol%), Et₃N (60 μ L), water (0.2 mL) and dioxane (1 mL) were stirred at r.t. for overnight. The compound was purified with over silica gel (DCM/MeOH, 0 \rightarrow 7 %) and obtained as yellow solid in 92% yield. ¹H NMR (300 MHz, DMSO) δ 7.88 (d, J = 7.7 Hz, 2H), 7.46 (d, J = 7.8 Hz, 2H), 6.89 (s, 1H), 6.36 (s, 1H), 5.74 (s, 1H), 4.36 (m, 1H), 3.60 – 3.39 (m, 3H), 3.27 (dd, J = 13.0, 7.7 Hz, 1H), 2.99 (s, 2H), 2.60 (s, 3H), 1.83 (s, 3H). ¹³C NMR (75 MHz, DMSO) δ 182.50, 172.58, 169.56, 163.11, 162.16, 160.11, 154.22, 142.82, 127.84, 127.52, 127.11, 124.89, 108.65, 104.49, 104.14, 99.11, 53.33, 52.65, 51.27, 44.12, 34.41, 27.86, 22.93; HR-ESIMS: m/z 511.1543 [M + H]⁺ (calcd for C₂₆H₂₇N₂O₇S, 511.1539).

4.2.2.7. (*S*)-methyl 2-((*tert*-butoxycarbonyl)amino)-3-((4-(5,7-dihydroxy-8-(1-methyl-1,2,3,6-tetrahydropyridin-4-yl)-4-oxo-4*H*-chromen-2-yl)phenyl)thio)propanoate (**12f**). **11a** (40 mg, 0.08 mmol), aminoacid (22 mg, 0.09 mmol), PdG3-Xantphos (6 mol%), Et₃N (60 μ L), and dioxane (1mL) were stirred at r.t. for overnight. The compound was purified with over silica gel (DCM/MeOH, 0 \rightarrow 7%) and obtained as orange solid in 86% yield. ¹H NMR (300 MHz, CDCl₃) δ 12.73 (s, 1H), 7.73 (d, J = 8.3 Hz, 2H), 7.49 (d, J = 8.3 Hz, 2H), 6.62 (s, 1H), 6.34 (s, 1H), 5.86 (s, 1H), 5.36 (s, 1H), 4.63 (s, 1H), 3.69 (s, 3H), 3.60 – 3.35 (m, 4H), 3.10 (q, J = 7.3 Hz, 2H), 3.00 (s, 2H), 2.68 (s, 3H), 1.43 (s, 9H). ¹³C NMR (75 MHz, CDCl₃) δ 182.41, 170.77, 162.66, 161.39, 161.18, 154.23, 140.80, 129.18, 128.91, 126.40, 125.89, 107.93, 105.11, 104.84, 99.63, 54.13, 53.27, 52.64, 52.22, 45.87, 44.86, 35.68, 28.91, 28.27, 8.74; ν_{\max} 1648, 1576,

1417, 1363, 1273, 1160, 1098, 1012, 826, 697, 627, 561, 484 cm⁻¹; HR-ESIMS: *m/z* 583.2110 [M + H]⁺ (calcd for C₃₀H₃₅N₂O₈S, 583.2114); HPLC purity, > 90% (*t_R* = 12.27 min).

4.2.2.8. 3-((4-(5,7-dihydroxy-8-(1-methyl-1,2,3,6-tetrahydropyridin-4-yl)-4-oxo-4H-chromen-2-yl)phenylthio)-N-((tetrahydro-2H-pyran-2-yl)oxy)propanamide (**12g**). **11a** (50 mg, 0.1 mmol), 3-mercapto-N-((tetrahydro-2H-pyran-2-yl)oxy)propanamide (23 mg, 0.11 mmol), PdG3-Xantphos (6 mol%), Et₃N (72 μL), and dioxane (1.5 mL) were stirred at r.t. for 2 h. The compound was purified on silica gel (DCM/MeOH, 0 → 7%) and obtained as orange solid in 76% yield. ¹H NMR (300 MHz, MeOD) δ 7.79 (d, *J* = 8.2 Hz, 2H), 7.43 (d, *J* = 8.3 Hz, 2H), 6.59 (s, 1H), 5.73 (s, 1H), 4.78 (1H overlapped with solvent signal), 3.99 (t, *J* = 10.2 Hz, 1H), 3.60 (d, *J* = 10.1 Hz, 1H), 3.45 – 3.22 (m, 6H), 2.93 (t, *J* = 5.3 Hz, 2H), 2.65 – 2.44 (m, 6H), 1.91 – 1.49 (m, 6H). ¹³C NMR (75 MHz, MeOD) δ 182.42, 168.61, 163.31, 162.98, 160.42, 154.23, 141.98, 128.26, 127.97, 127.40, 126.41, 125.20, 108.58, 103.59, 101.91, 61.64, 53.74, 51.65, 43.83, 31.96, 28.28, 27.56, 27.20, 24.80, 18.04; *v*_{max} 1645, 1410, 1373, 1202, 1101, 1065, 1036, 896, 819, 749, 699, 621, 561 cm⁻¹; HR-ESIMS: *m/z* 553.2015 [M + H]⁺ (calcd for C₂₉H₃₃N₂O₇S, 553.2008); HPLC purity, >90% (*t_R* = 10.54 min).

4.2.2.9. 3-((4-(5,7-dihydroxy-8-(1-methyl-1,2,3,6-tetrahydropyridin-4-yl)-4-oxo-4H-chromen-2-yl)phenylthio)-N-hydroxypropanamide (**12h**). To a mixture of **12g** in dioxane was added dropwise HCl in dioxane 4M (0.6 mL) and the mixture stirred for 30 minutes at r.t. the solvent was removed under vacuum. the product was purified by HPLC (water/ACN) to yield a yellow powder (81%). ¹H NMR (300 MHz, D₂O) δ 8.37 (s, 1H), 7.04 (d, *J* = 5.6 Hz, 2H), 6.93 (d, *J* = 8.2 Hz, 2H), 6.00 (s, 1H), 5.89 (s, 1H), 5.39 (s, 1H), 3.00 (d, *J* = 23.6 Hz, 5H), 2.43 (s, 4H); *v*_{max} 2971, 2900, 1648, 1561, 1409, 1366, 1273, 1187, 1066, 824, 770, 628, 558 cm⁻¹; HR-ESIMS: *m/z* 469.1432 [M + H]⁺ (calcd for C₂₄H₂₅N₂O₆S, 469.1433); HPLC purity, > 90% (*t_R* = 9.34 min).

4.2.2.10. 2-(4-((1H-benzo[d]imidazol-2-yl)thio)phenyl)-5,7-dihydroxy-8-(1-methyl-1,2,3,6-tetrahydropyridin-4-yl)-4H-chromen-4-one (**12j**). **11a** (30 mg, 0.063 mmol), 1H-benzo[d]imidazole-2-thiol (10 mg, 0.069 mmol), PdG3-Xantphos (8 mol%), Et₃N (60 μL), water (200 μL) and dioxane (1 mL) were stirred overnight at 60°C. The compound was purified on silica gel (DCM/MeOH, 0 → 7%) and obtained as orange solid in 66% yield. ¹H NMR (400 MHz, DMSO) δ 12.66 (s, 1H), 7.80 (d, *J* = 7.5 Hz, 2H), 7.54 – 7.27 (m, 4H), 7.04 (d, *J* = 3.0 Hz, 2H), 6.77 (s, 1H), 6.13 (s, 1H), 5.55 (m, 2H), 2.98 (d, *J* = 16.2 Hz, 2H), 2.33 (s, 4H), 2.19 (s, 3H). ¹³C NMR (101 MHz, DMSO) δ 182.13, 162.17, 159.78, 153.84, 144.98, 136.76, 130.41, 130.13, 127.13, 126.12, 122.40, 109.01, 104.86, 103.72, 98.78, 54.88, 54.12, 51.68, 45.09, 28.85; *v*_{max} 1655, 1581, 1402, 1363, 1270, 829, 743, 560, 512, 495, 477 cm⁻¹; HR-ESIMS: *m/z* 498.1494 [M + H]⁺ (calcd for C₂₈H₂₄N₃O₄S, 498.1488); HPLC purity, 100% (*t_R* = 10 min).

4.2.2.11. 2-(4-(benzo[d]oxazol-2-ylthio)phenyl)-5,7-dihydroxy-8-(1-methyl-1,2,3,6-tetrahydropyridin-4-yl)-4H-chromen-4-one (**12k**). **11a** (30 mg, 0.063 mmol), benzo[d]oxazole-2-thiol (12 mg, 0.075 mmol), PdG3-Xantphos (10 mol%), Et₃N (70 μL), and dioxane (1 mL) were stirred 2 hours at 60 °C. The compound was purified on silica gel (DCM/MeOH, 0 → 5%) and obtained as yellow solid in 60% yield. ¹H NMR (400 MHz, DMSO) δ 12.93 (s, 1H), 8.12 (d, *J* = 7.7 Hz, 2H), 7.94 (s, 2H), 7.69 (s, 2H), 7.39 (d, *J* = 2.9 Hz, 3H), 7.11 (s, 1H), 6.37 (s, 1H), 5.86 (s, 1H), 2.88 (s, 4H), 2.65 (s, 3H), 2.55 (overlapped with solvent). ¹³C NMR (101 MHz, DMSO) δ 182.10, 161.99, 161.75, 160.30, 153.86, 151.37, 133.95, 131.91, 127.63, 125.13, 124.93, 122.23, 118.92, 110.53, 107.17, 105.67, 99.53, 98.69, 51.60, 50.05, 42.16, 25.74; HR-ESIMS: *m/z* 499.1333 [M + H]⁺ (calcd for C₂₈H₂₃NO₅S, 499.1328); HPLC purity, >90% (*t_R* = 12.31 min).

4.2.2.12. 5,7-dihydroxy-2-(4-((5-methoxy-1H-benzo[d]imidazol-2-yl)thio)phenyl)-8-(1-methyl-1,2,3,6-tetrahydropyridin-4-yl)-4H-chromen-4-one (**12l**). **11a** (30 mg, 0.063 mmol), 6-methoxy-1H-benzo[d]imidazole-2-thiol (14 mg, 0.075 mmol), PdG3-Xantphos (10 mol%), Et₃N (70 μL), and dioxane (1 mL) were stirred overnight at 60°C. The compound was purified on silica gel (DCM/MeOH, 0 → 7%) and obtained as yellow solid in 30% yield. ¹H NMR (300 MHz, MeOD) δ 7.93 (d, *J* = 7.9 Hz, 2H), 7.61 – 7.39 (m, 3H), 7.06 (s, 1H), 6.95 (d, *J* = 8.9 Hz, 1H), 6.78 (s, 1H), 6.30 (s, 1H), 5.84 (s, 1H), 3.85 (s, 3H), 3.81 (s, 2H), 3.33 (overlapped with solvent), 2.89 (s, 3H), 2.74 (s, 2H). ¹³C NMR (101 MHz, DMSO) δ 182.12, 162.49, 160.27, 153.83, 129.55, 127.37, 122.49, 112.27, 104.93, 103.87, 98.69, 55.51, 51.70, 50.11, 42.35, 25.97; *v*_{max} 1650, 1403, 1100, 829, 698, 529, 511, 494, 487, 477, 460, 452 cm⁻¹; HR-ESIMS: *m/z* 528.1594 [M + H]⁺ (calcd for C₂₉H₂₆N₃O₅S, 528.1593); HPLC purity, 94.10% (*t_R* = 10.08 min).

4.2.2.13. 5,7-dihydroxy-8-(1-methyl-1,2,3,6-tetrahydropyridin-4-yl)-2-(4-(pyrimidin-2-ylthio)phenyl)-4H-chromen-4-one (**12m**). **11a** (30 mg, 0.063 mmol), pyrimidine-2-thiol (10 mg, 0.075 mmol), PdG3-Xantphos (6 mol%), Et₃N (100 μL), and dioxane (1 mL) were stirred overnight at 60°C. The compound was purified on silica gel (DCM/MeOH, 0 → 7%) and obtained as yellow solid in 69% yield. ¹H NMR (300 MHz, MeOD) δ 8.56 (d, *J* = 5.0 Hz, 2H), 8.04 (d, *J* = 8.5 Hz, 2H), 7.84 (d, *J* = 7.7 Hz, 2H), 7.21 (m, 1H), 6.87 (s, 1H), 6.33 (s, 1H), 5.91 (s, 1H), 3.85 (s, 2H), 3.34 (overlapped with solvent), 2.92 (s, 3H), 2.79 (s, 2H). ¹³C NMR (75 MHz, MeOD) δ 157.73, 135.22, 126.68, 123.70, 117.73, 110.29, 105.00, 99.29, 53.15, 51.07, 43.00, 27.37; *v*_{max} 2976, 1649, 1561, 1405, 1371, 1276, 1248, 1186, 1100, 1014, 834, 768,

562 cm⁻¹; HR-ESIMS: *m/z* 460.1325 [M + H]⁺ (calcd for C₂₅H₂₂N₃O₄S, 460.1331); HPLC purity, 100% (*t_R* = 11.33 min).

4.2.2.13. 5,7-dihydroxy-8-(1-methyl-1,2,3,6-tetrahydropyridin-4-yl)-2-(4-((5-phenyl-1H-imidazol-2-yl)thio)phenyl)-4H-chromen-4-one (**12n**). **11a** (20 mg, 0.042 mmol), 5-phenyl-1H-imidazole-2-thiol (9 mg, 0.05 mmol), PdG3-Xantphos (6 mol%), Et₃N (50 μL), and dioxane (1 mL) were stirred overnight at 60 °C. The compound was purified on silica gel (DCM/MeOH, 0 → 10 %) and obtained as yellow solid in 68% yield. ¹H NMR (300 MHz, MeOD) δ 7.88 (d, *J* = 7.9 Hz, 2H), 7.76 (d, *J* = 7.3 Hz, 2H), 7.68 (s, 1H), 7.47 – 7.24 (m, 5H), 6.73 (s, 1H), 6.28 (s, 1H), 5.81 (s, 1H), 3.73 (s, 2H), 3.33, (2H overlapped with solvent), 2.83 (s, 3H), 2.70 (s, 2H). ¹³C NMR (75 MHz, MeOD) δ 182.52, 163.35, 162.32, 161.07, 154.44, 141.27, 129.14, 128.46, 127.12, 126.89, 124.53, 122.83, 104.33, 98.66, 52.67, 51.02, 42.52, 26.79; *v*_{max} 1647, 1570, 1412, 1362, 1274, 1099, 829, 761, 691, 558, 530, 495, 477, 460 cm⁻¹; HR-ESIMS: *m/z* 524.1647 [M + H]⁺ (calcd for C₃₀H₂₅N₃O₄S, 524.1644); HPLC purity, 96 % (*t_R* = 10.18 min).

4.2.2.14. 5,7-dihydroxy-8-(1-methyl-1,2,3,6-tetrahydropyridin-4-yl)-2-(4-((1-methyl-1H-benzo[d]imidazol-2-yl)thio)phenyl)-4H-chromen-4-one (**12o**). **11a** (25 mg, 0.052 mmol), 1-methyl-1H-benzo[d]imidazole-2-thiol (10 mg, 0.057 mmol), PdG3-Xantphos (7 mol%), Et₃N (50 μL), and dioxane (1 mL) were stirred 4 hours at 60°C. The compound was purified on silica gel (DCM/MeOH, 0 → 10%) and obtained as yellow solid in 60 % yield. ¹H NMR (300 MHz, MeOD) δ 7.91 (d, *J* = 8.0 Hz, 2H), 7.70 (d, *J* = 7.9 Hz, 2H), 7.58 (d, *J* = 7.8 Hz, 1H), 7.51 – 7.27 (m, 5H), 6.73 (s, 1H), 5.79 (s, 1H), 3.88 (s, 3H), 3.63 (s, 2H), 3.20 (t, *J* = 5.6 Hz, 2H), 2.76 (s, 3H), 2.66 (s, 2H). ¹³C NMR (75 MHz, MeOD) δ 162.93, 142.01, 137.42, 136.34, 130.22, 129.09, 127.19, 123.89, 123.33, 122.91, 118.47, 110.28, 104.62, 52.87, 51.14, 42.81, 30.10, 27.11; *v*_{max} 1576, 1404, 1363, 1274, 1097, 1010, 829, 743, 558, 540, 529, 512, 495, 477, 460 cm⁻¹; HR-ESIMS: *m/z* 512.1649 [M + H]⁺ (calcd for C₂₉H₂₆N₃O₄S, 512.1644); HPLC purity, 96.03 % (*t_R* = 10.94 min).

4.2.2.15. 5,7-dihydroxy-8-(1-methyl-1,2,3,6-tetrahydropyridin-4-yl)-2-(4-(quinolin-2-ylthio)phenyl)-4H-chromen-4-one (**12p**). **11a** (30 mg, 0.063 mmol), quinoline-2-thiol (13 mg, 0.075 mmol), PdG3-Xantphos (7 mol%), Et₃N (50 μL), and dioxane (1 mL) were stirred 4 hours at 60°C. The compound was purified on silica gel (DCM/MeOH, 0 → 10 %) and obtained as yellow solid in 70% yield. ¹H NMR (400 MHz, DMSO) δ 12.92 (s, 1H), 8.26 (s, 1H), 8.17 – 7.64 (m, 8H), 7.54 (s, 1H), 7.27 (s, 1H), 7.01 (s, 1H), 6.35 (s, 1H), 5.84 (s, 1H), 3.91 (s, 2H), 3.42 (s, 2H), 2.90 (s, 3H), 2.65 (s, 2H). ¹³C NMR (101 MHz, DMSO) δ 182.55, 162.66, 162.18, 160.78, 158.91, 154.27, 147.95, 137.80, 135.46, 134.69, 131.41, 130.87, 128.50, 128.13, 127.84, 126.75, 126.44, 122.61, 120.86, 107.70, 105.73, 104.39, 99.16, 52.07, 50.55, 42.62, 26.19; HR-ESIMS: *m/z* 509.1530 [M + H]⁺ (calcd for C₃₀H₂₅N₃O₄S, 509.1535); HPLC purity, 98.39 % (*t_R* = 12.56 min).

4.2.2.16. 6-((4-(5,7-dihydroxy-8-(1-methyl-1,2,3,6-tetrahydropyridin-4-yl)-4-oxo-4H-chromen-2-yl)phenyl)thio)-N-hydroxynicotinamide (**12q**). **11a** (30 mg, 0.063 mmol), 6-mercapto-N-((tetrahydro-2H-pyran-2-yl)oxy)nicotinamide (18 mg, 0.069 mmol), PdG3-Xantphos (10 mol%), Et₃N (50 μL), and dioxane (1mL) were stirred at r.t. for 2 h. To a solution of the crude compound (30 mg, 0.05 mmol) in dioxane (1 mL) was added dropwise HCl in dioxane 4M (0.4 mL) and the mixture stirred for 60 minutes at r.t. the solvent was removed under vacuum. The product was purified by HPLC (water/ACN) to yield a yellow powder (30%). ¹H NMR (300 MHz, DMSO) δ 12.86 (s, 1H), 8.74 (s, 1H), 8.21 (s, 1H), 8.09 (d, *J* = 8.2 Hz, 2H), 8.01 (dd, *J* = 8.3, 1.8 Hz, 1H), 7.78 (d, *J* = 8.2 Hz, 2H), 7.25 (d, *J* = 8.3 Hz, 1H), 7.06 (s, 1H), 6.35 (s, 1H), 5.76 (s, 1H), 3.30 (s, 2H), 2.83 (d, *J* = 5.1 Hz, 2H), 2.48 (s, 5H). ¹³C NMR (75 MHz, DMSO) δ 182.62, 164.15, 162.42, 161.99, 154.32, 148.51, 136.44, 135.06, 134.75, 131.97, 127.83, 125.88, 121.90, 109.15, 105.82, 104.28, 99.17, 54.00, 51.75, 44.92, 28.68; *v*_{max} 2987, 2900, 1652, 1578, 1403, 1371, 1275, 1189, 1066, 832, 770, 746, 628, 562, 528 cm⁻¹; *m/z* 518.1386 [M + H]⁺ (calcd for C₂₇H₂₄N₃O₆S⁺, 518.1386); HPLC purity, 100% (*t_R* = 9.38 min).

4.2.2.17. 6-((4-(5,7-dihydroxy-8-(1-methyl-1,2,3,6-tetrahydropyridin-4-yl)-4-oxo-4H-chromen-2-yl)phenyl)thio)nicotinic acid (**12r**). **11a** (20 mg, 0.042 mmol), 6-mercaptonicotinic acid (8 mg, 0.05 mmol), PdG3-Xantphos (7 mol%), Et₃N (50 μL), and dioxane (1 mL) were stirred 2 hours at 60°C. The compound was purified with HPLC (gradient ACN in water) and obtained as yellow solid in 47% yield. ¹H NMR (400 MHz, DMSO) δ 12.78 (s, 1H), 8.82 (s, 1H), 8.20 (s, 1H), 8.01 (m, 2H), 7.91 (m, 1H), 7.69 (m, 2H), 7.12 (s br, 1H), 6.96 (d, *J* = 21.1 Hz, 1H), 6.27 (d, *J* = 5.7 Hz, 1H), 5.67 (s, 1H), 2.6 (signals overlapping with solvents), 2.34 (s, 3H). *v*_{max} 1605, 1577, 1419, 1401, 1346, 1275, 1096, 833, 787, 697, 563, 527, 488, 461 cm⁻¹; HR-ESIMS: *m/z* 503.1276 [M + H]⁺ (calcd for C₂₇H₂₃N₂O₆S, 503.1277); HPLC purity, >90% (*t_R* = 10.94 min).

4.2.2.18. 5,7-dihydroxy-8-(1-methyl-1,2,3,6-tetrahydropyridin-4-yl)-2-(4-(phenylamino)phenyl)-4H-chromen-4-one (**12s**). **11a** (20 mg, 0.042 mmol), aniline (8 mg, 0.082 mmol), PdG3-Xantphos (10 mol%), Cs₂CO₃ (20 mg, 0.062 mmol) and dioxane (1 mL) were stirred overnight at 100°C. The compound was purified with HPLC, yield 35 % . ¹H NMR (400 MHz, DMSO) δ 13.40 (s, 1H), 11.07 (s, 1H), 9.00 (s, 1H), 7.77 (m, 2H), 7.40 – 7.05 (m, 5H), 6.91 (m, 1H), 6.69 (m, 1H), 6.43 (s, 1H), 5.77 (s, 1H), 3.16 (s, 5H), 2.89 (s, 2H), 2.54 (s, 2H). ¹³C NMR (101 MHz, DMSO) δ 181.85,

163.99, 161.28, 160.24, 153.67, 147.66, 141.32, 129.27, 129.02, 128.33, 127.59, 121.77, 121.63, 119.88, 119.30, 115.05, 114.66, 106.86, 103.48, 101.63, 98.55, 50.88, 49.44, 48.54, 41.59, 25.29; HR-ESIMS: m/z 441.1811 [M + H]⁺ (calcd for C₂₇H₂₅N₂O₄, 441.1814).

4.2.2.19. 2-(4-((1*H*-benzo[d]imidazol-2-yl)thio)-2-chlorophenyl)-5,7-dihydroxy-8-(1-methyl-1,2,3,6-tetrahydropyridin-4-yl)-4*H*-chromen-4-one (**13b**). **11b** (30 mg, 0.059 mmol), 1*H*-benzo[d]imidazole-2-thiol (10 mg, 0.064 mmol), PdG3-Xantphos (10 mol%), Et₃N (70 μL), and dioxane (1 mL) were stirred overnight at 60°C. The compound was purified on silica gel (DCM/MeOH, 0 → 5%) and obtained as yellow solid in 60% yield. ¹H NMR (400 MHz, DMSO) δ 13.18 (s, 1H), 12.77 (s, 1H), 7.77 (d, *J* = 8.2 Hz, 2H), 7.63 – 7.50 (m, 3H), 7.25 (dd, *J* = 5.8, 2.9 Hz, 2H), 6.62 (s, 1H), 6.41 (s, 1H), 5.66 (s, 1H), 3.23 (s, 2H), 2.80 (s, 2H), 2.47 – 2.36 (m, 5H). ¹³C NMR (101 MHz, DMSO) δ 181.67, 161.94, 159.94, 154.34, 143.89, 137.98, 132.21, 130.49, 129.63, 128.43, 126.78, 124.96, 108.69, 103.67, 52.85, 51.04, 43.70, 28.04; ν_{\max} 1651, 1573, 1413, 1360, 1276, 1099, 743, 539, 530, 505, 495, 477, 460 cm⁻¹; HR-ESIMS: m/z 532.1104 [M + H]⁺ (calcd for C₂₈H₂₃N₃O₄SCl, 532.1098); HPLC purity, > 90% (*t*_R = 8.92 min).

4.2.2.20. 2-(2-chloro-4-((1-methyl-1*H*-benzo[d]imidazol-2-yl)thio)phenyl)-5,7-dihydroxy-8-(1-methyl-1,2,3,6-tetrahydropyridin-4-yl)-4*H*-chromen-4-one (**13c**). **11b** (20 mg, 0.04 mmol), 1-methyl-1*H*-benzo[d]imidazole-2-thiol (10 mg, 0.043 mmol), PdG3-Xantphos (10 mol%), Et₃N (50 μL), and dioxane (1 mL) were stirred 2 hours at 60°C. The compound was purified on silica gel (DCM/MeOH, 3 → 5%) and obtained as yellow solid in 60% yield. ¹H NMR (300 MHz, MeOD) δ 7.81 – 7.52 (m, 4H), 7.50 – 7.28 (m, 2H), 6.55 (s, 1H), 6.37 (s, 1H), 5.79 (s, 1H), 4.02 – 3.73 (m, 5H), 3.34 – 3.33 (m, 2H), 2.92 (m, 3H), 2.73 (s, 2H). ¹³C NMR (75 MHz, MeOD) δ 162.64, 154.74, 138.17, 133.20, 130.05, 127.61, 124.02, 123.02, 121.31, 118.52, 110.53, 110.37, 98.63, 51.87, 50.49, 41.43, 30.13, 25.72; ν_{\max} 1651, 1574, 1414, 1360, 1276, 1186, 1099, 820, 761, 743, 540, 530, 495, 477, 460 cm⁻¹; HR-ESIMS: m/z 546.1255 [M + H]⁺ (calcd for C₂₉H₂₅N₃O₄SCl⁺, 546.1254); HPLC purity, 91 % (*t*_R = 11.02min).

4.2.2.21. 2-(2-chloro-4-(pyrimidin-2-ylthio)phenyl)-5,7-dihydroxy-8-(1-methyl-1,2,3,6-tetrahydropyridin-4-yl)-4*H*-chromen-4-one (**13d**). **11b** (20 mg, 0.04 mmol), pyrimidine-2-thiol (15 mg, 0.043 mmol), PdG3-Xantphos (10 mol%), Et₃N (50 μL), and dioxane (2 mL) were stirred 2 hours at 60°C. The compound was purified on silica gel (DCM/MeOH, 0 → 5%) and obtained as yellow solid in 65% yield. ¹H NMR (300 MHz, MeOD) δ 8.60 (d, *J* = 4.7 Hz, 2H), 7.90 (s, 1H), 7.75 (s, 2H), 7.25 (d, *J* = 4.6 Hz, 1H), 6.55 (s, 1H), 6.31 (s, 1H), 5.78 (s, 1H), 3.52 (s, 2H), 3.11 (s, 2H), 2.65 (d, *J* = 16.7 Hz, 5H). ¹³C NMR (75 MHz, MeOD) δ 172.91, 157.85, 136.00, 134.70, 133.38, 132.48, 131.15, 128.22, 123.68, 117.99, 110.42, 108.32, 99.16, 52.93, 51.05, 42.73, 27.30; ν_{\max} 2987, 2900, 1651, 1557, 1409, 1376, 1259, 1183, 1100, 1057, 803, 769, 629, 549 cm⁻¹; ESIMS: m/z 494.0943 [M + H]⁺ (calcd for C₂₅H₂₁ClN₃O₄S, 494.0941); HPLC purity, 96% (*t*_R = 10.49 min).

4.3. Biology

4.3.1. Cell culture and proliferation assay

Cancer cell lines were obtained from the American type Culture Collection (Rockville, USA) and were cultured according to the supplier's instructions. U87-MG cells were grown in Dulbecco minimal essential medium (DMEM) containing 4.5 g/L glucose supplemented with 10% FCS and 1% glutamine. All cell lines were maintained at 37°C in a humidified atmosphere containing 5% CO₂. Cell viability was assessed using Promega CellTiter-Blue reagent according to the manufacturer's instructions. Cells were seeded in 96-well plates (5 X 10³ cells per well) containing 50 μL growth medium. After 24 h of culture, the cells were supplemented with 50 μL of the test compound dissolved in DMSO (less than 0.1% in each preparation). After 72 h of incubation, 20 μL of resazurin was added for 2 h before recording fluorescence (λ_{ex} = 560 nm, λ_{em} = 590 nm) using a Victor microtiter plate fluorimeter (Perkin-Elmer, USA). The IC₅₀ value corresponds to the concentration of test compound that caused a decrease of 50% in fluorescence of drug-treated cells compared with untreated cells. Experiments were performed in triplicate.

4.3.2. Protein kinase assays

Kinase activities were measured according to the Promega's ADP-Glo assay described in Nguyen et al[49] except for the following enzymes: (i) *Lm*CK1 (from *Leishmania major*, recombinant, expressed in bacteria) was assayed in buffer A with 0.028 μg/μl of the following peptide: RRKHAAIGSpAYSITA as CK1-specific substrate; (ii) *Pf*GSK3 (for *Plasmodium falciparum*, recombinant, expressed in bacteria) was assayed in buffer A with 0.010 μg/μl of GS-1 peptide, a GSK3-selective substrate (YRRAAVPPSPSLSRHSSPHQSpEDEEE); (iii) *Ssc*CK1δ/ε (casein kinase 1δ/ε, porcine

brain, native, affinity purified) was assayed in buffer A with 0.022 $\mu\text{g}/\mu\text{l}$ of the following peptide: RRKHAAlGSpAYSITA (“Sp” stands for phosphorylated serine) as CK1-specific substrate; (iv) *Ssc*GSK3 α/β (glycogen synthase kinase 3, porcine brain, native, affinity purified) isoforms were assayed in buffer A with 0.010 $\mu\text{g}/\mu\text{l}$ of GS-1 peptide, a GSK3-selective substrate (YRRAAVPPSPSLSRHSSPHQSpEDEEE). The buffer solution A used in this study is composed of 10 mM MgCl_2 , 1 mM EGTA, 1 mM DTT, 25 mM Tris-HCl pH 7.5 and 50 $\mu\text{g}/\text{ml}$ heparin.

4.3.3. ATP competition assay

The activity of *Hs*GSK3 β was measured according to the Promega’s ADP-Glo assay described in Nguyen et al (Ref). Assays were performed in the absence or presence of (ni147)**13c** at 500 nM and increasing doses of ATP (from 3.125 to 100 μM). To plot and analyze the data, we used the software Prism-GraphPad (GraphPad Software, San Diego, CA, USA).

Acknowledgments

The authors acknowledge support of this project by the CNRS and University Paris-Sud and “La Ligue Contre le Cancer” throughout an “Equipe Labellisée 2014” grant. Our laboratory is a member of the Laboratory of Excellence LERMIT supported by a grant (ANR-10-LABX-33). The authors also thank the Cancéropôle Grand Ouest (“Marines molecules, metabolism and cancer” network), IBiSA (French Infrastructures en sciences du vivant: biologie, santé et agronomie) and Biogenouest (Western France life science and environment core facility network) for supporting the KISSf screening facility (FR2424, CNRS and Sorbonne Université), Roscoff, France.

Appendix A. Supplementary data

Supplementary data to this article can be found online at <https://doi.org/>

References

- [1] K.C. Nicolaou, J.A. Pfefferkorn, A.J. Roecker, G.Q. Cao, S. Barluenga, H.J. Mitchell, Natural Product-like Combinatorial Libraries Based on Privileged Structures. 1. General Principles and Solid-Phase Synthesis of Benzopyrans, *J. Am. Chem. Soc.*, 122 (2000) 9939-9953.
- [2] F. Pojero, P. Poma, V. Spanò, A. Montalbano, P. Barraja, M. Notarbartolo, Targeting multiple myeloma with natural polyphenols, *Eur. J. Med. Chem.*, 180 (2019) 465-485.
- [3] L. Jalili-Baleh, E. Babaei, S. Abdpour, S. Nasir Abbas Bukhari, A. Foroumadi, A. Ramazani, M. Sharifzadeh, M. Abdollahi, M. Khoobi, A review on flavonoid-based scaffolds as multi-target-directed ligands (MTDLs) for Alzheimer's disease, *Eur. J. Med. Chem.*, 152 (2018) 570-589.
- [4] R. Kshatriya, V.P. Jejurkar, S. Saha, In memory of Prof. Venkataraman: Recent advances in the synthetic methodologies of flavones, *Tetrahedron*, 74 (2018) 811-833.
- [5] X. Zi, D.K. Feyes, R. Agarwal, Anticarcinogenic effect of a flavonoid antioxidant, silymarin, in human breast cancer cells MDA-MB 468: induction of G1 arrest through an increase in Cip1/p21 concomitant with a decrease in kinase activity of cyclin-dependent kinases and associated cyclins, *Clin. Cancer Res.*, 4 (1998) 1055-1064.

- [6] S. Saisomboon, R. Kariya, K. Vaeteewoottacharn, S. Wongkham, K. Sawanyawisuth, S. Okada, Antitumor effects of flavopiridol, a cyclin-dependent kinase inhibitor, on human cholangiocarcinoma in vitro and in an in vivo xenograft model, *Heliyon*, 5 (2019) e01675.
- [7] J. Wang, T. Li, T. Zhao, T. Wu, C. Liu, H. Ding, Z. Li, J. Bian, Design of wogonin-inspired selective cyclin-dependent kinase 9 (CDK9) inhibitors with potent in vitro and in vivo antitumor activity, *Eur. J. Med. Chem.*, 178 (2019) 782-801.
- [8] A.M. Senderowicz, Development of cyclin-dependent kinase modulators as novel therapeutic approaches for hematological malignancies, *Leukemia*, 15 (2001) 1-9.
- [9] R. Roskoski, Properties of FDA-approved small molecule protein kinase inhibitors, *Pharmacol Res.*, 144 (2019) 19-50.
- [10] I. Neant, P. Guerrier, 6-Dimethylaminopurine blocks starfish oocyte maturation by inhibiting a relevant protein kinase activity, *Exp. Cell Res.*, 176 (1988) 68-79.
- [11] J. Veselý, L. Havlíček, M. Strnad, J.J. Blow, A. Donella-Deana, L. Pinna, D.S. Letham, J.-y. Kato, L. Detivaud, S. Leclerc, L. Meijer, Inhibition of Cyclin-Dependent Kinases by Purine Analogues, *Eur. J. Biochem.*, 224 (1994) 771-786.
- [12] L. Meijer, A. Borgne, O. Mulner, J.P.J. Chong, J.J. Blow, N. Inagaki, M. Inagaki, J.-G. Delcros, J.-P. Moulinoux, Biochemical and Cellular Effects of Roscovitine, a Potent and Selective Inhibitor of the Cyclin-Dependent Kinases *cdc2*, *cdk2* and *cdk5*, *Eur. J. Biochem.*, 243 (1997) 527-536.
- [13] Y. Teng, K. Lu, Q. Zhang, L. Zhao, Y. Huang, A.M. Ingarrá, H. Galons, T. Li, S. Cui, P. Yu, N. Oumata, Recent advances in the development of cyclin-dependent kinase 7 inhibitors, *Eur. J. Med. Chem.*, 183 (2019) 111641.
- [14] L. Demange, F.N. Abdellah, O. Lozach, Y. Ferandin, N. Gresh, L. Meijer, H. Galons, Potent inhibitors of CDK5 derived from roscovitine: Synthesis, biological evaluation and molecular modelling, *Bioorg. Med. Chem. Lett.*, 23 (2013) 125-131.
- [15] N.S. Gray, L. Wodicka, A.-M.W.H. Thunnissen, T.C. Norman, S. Kwon, F.H. Espinoza, D.O. Morgan, G. Barnes, S. LeClerc, L. Meijer, S.-H. Kim, D.J. Lockhart, P.G. Schultz, Exploiting Chemical Libraries, Structure, and Genomics in the Search for Kinase Inhibitors, *Science*, 281 (1998) 533-538.
- [16] H.-K. Wang, The therapeutic potential of flavonoids, *Expert. Opin. Investig. Drugs.*, 9 (2000) 2103-2119.
- [17] S. Zhang, J. Ma, Y. Bao, P. Yang, L. Zou, K. Li, X. Sun, Nitrogen-containing flavonoid analogues as CDK1/cyclin B inhibitors: Synthesis, SAR analysis, and biological activity, *Bioorg. Med. Chem.*, 16 (2008) 7127-7132.
- [18] M.R. Vijayababu, P. Kanagaraj, A. Arunkumar, R. Ilangovan, M.M. Aruldas, J. Arunakaran, Quercetin-induced growth inhibition and cell death in prostatic carcinoma cells (PC-3) are associated with increase in p21 and hypophosphorylated retinoblastoma proteins expression, *J. Cancer. Res. Clin. Oncol.*, 131 (2005) 765-771.
- [19] A.D. Harmon, U. Weiss, J.V. Silverton, The structure of rohitukine, the main alkaloid of *Amoora rohituka* (*Syn. Aphanamixis polystachya*) (*meliaceae*), *Tetrahedron Lett.*, 20 (1979) 721-724.
- [20] R.G. Naik, S.L. Kattige, S.V. Bhat, B. Alreja, N.J. de Souza, R.H. Rupp, An antiinflammatory cum immunomodulatory piperidinylbenzopyranone from *Dysoxylum binectariferum* : isolation, structure and total synthesis, *Tetrahedron*, 44 (1988) 2081-2086.
- [21] V. Kumar, S.K. Guru, S.K. Jain, P. Joshi, S.G. Gandhi, S.B. Bharate, S. Bhushan, S.S. Bharate, R.A. Vishwakarma, A chromatography-free isolation of rohitukine from leaves of *Dysoxylum binectariferum*: Evaluation for in vitro cytotoxicity, Cdk inhibition and physicochemical properties, *Bioorg. Med. Chem. Lett.*, 26 (2016) 3457-3463.

- [22] A. Singh, P. Chibber, P. Kolimi, T.A. Malik, N. Kapoor, A. Kumar, N. Kumar, S.G. Gandhi, S. Singh, S.T. Abdullah, R. Vishwakarma, G. Singh, Rohitukine inhibits NF- κ B activation induced by LPS and other inflammatory agents, *Int. Immunopharmacol.*, 69 (2019) 34-49.
- [23] M.C. Lanasa, L. Andritsos, J.R. Brown, J. Gabrilove, F. Caligaris-Cappio, P. Ghia, R.A. Larson, T.J. Kipps, V. Leblond, D.W. Milligan, A. Janssens, A.J. Johnson, N.A. Heerema, A. Bühler, S. Stilgenbauer, J. Devin, M. Hallek, J.C. Byrd, M.R. Grever, Final results of EFC6663: A multicenter, international, phase 2 study of alvocidib for patients with fludarabine-refractory chronic lymphocytic leukemia, *Leuk. Res.*, 39 (2015) 495-500.
- [24] T.S. Lin, A.S. Ruppert, A.J. Johnson, B. Fischer, N.A. Heerema, L.A. Andritsos, K.A. Blum, J.M. Flynn, J.A. Jones, W. Hu, M.E. Moran, S.M. Mitchell, L.L. Smith, A.J. Wagner, C.A. Raymond, L.J. Schaaf, M.A. Phelps, M.A. Villalona-Calero, M.R. Grever, J.C. Byrd, Phase II Study of Flavopiridol in Relapsed Chronic Lymphocytic Leukemia Demonstrating High Response Rates in Genetically High-Risk Disease, *J. Clin. Oncol.*, 27 (2009) 6012-6018.
- [25] J.F. Zeidner, M.C. Foster, A.L. Blackford, M.R. Litzow, L.E. Morris, S.A. Strickland, J.E. Lancet, P. Bose, M.Y. Levy, R. Tibes, I. Gojo, C.D. Gocke, G.L. Rosner, R.F. Little, J.J. Wright, L.A. Doyle, B.D. Smith, J.E. Karp, Randomized multicenter phase II study of flavopiridol (alvocidib), cytarabine, and mitoxantrone (FLAM) versus cytarabine/daunorubicin (7+3) in newly diagnosed acute myeloid leukemia, *Haematologica*, 100 (2015) 1172-1179.
- [26] Y.-Y. Yeh, R. Chen, J. Hessler, E. Mahoney, A.M. Lehman, N.A. Heerema, M.R. Grever, W. Plunkett, J.C. Byrd, A.J. Johnson, Up-regulation of CDK9 kinase activity and Mcl-1 stability contributes to the acquired resistance to cyclin-dependent kinase inhibitors in leukemia, *Oncotarget*, 6 (2014) 2667-2679.
- [27] R. Chen, W.G. Wierda, S. Chubb, R.E. Hawtin, J.A. Fox, M.J. Keating, V. Gandhi, W. Plunkett, Mechanism of action of SNS-032, a novel cyclin-dependent kinase inhibitor, in chronic lymphocytic leukemia, *Blood*, 113 (2009) 4637-4645.
- [28] Y. Li, K. Tanaka, X. Li, T. Okada, T. Nakamura, M. Takasaki, S. Yamamoto, Y. Oda, M. Tsuneyoshi, Y. Iwamoto, Cyclin-dependent kinase inhibitor, flavopiridol, induces apoptosis and inhibits tumor growth in drug-resistant osteosarcoma and Ewing's family tumor cells, *Int. J. Cancer*, 121 (2007) 1212-1218.
- [29] P.H. Wiernik, Alvocidib (flavopiridol) for the treatment of chronic lymphocytic leukemia, *Expert Opin. Investig. Drugs*, 25 (2016) 729-734.
- [30] J.F. Zeidner, J.E. Karp, Clinical activity of alvocidib (flavopiridol) in acute myeloid leukemia, *Leuk. Res.*, 39 (2015) 1312-1318.
- [31] S.B. Bharate, V. Kumar, S.K. Jain, M.J. Mintoo, S.K. Guru, V.K. Nuthakki, M. Sharma, S.S. Bharate, S.G. Gandhi, D.M. Mondhe, S. Bhushan, R.A. Vishwakarma, Discovery and Preclinical Development of IIM-290, an Orally Active Potent Cyclin-Dependent Kinase Inhibitor, *J. Med. Chem.*, 61 (2018) 1664-1687.
- [32] S. K. Jain, S. B. Bharate, R. A. Vishwakarma, Cyclin-Dependent Kinase Inhibition by Flavoalkaloids, *Mini Rev. Med. Chem.*, 12 (2012) 632-649.
- [33] R.D. Cassaday, A. Goy, S. Advani, P. Chawla, R. Nachankar, M. Gandhi, A.K. Gopal, A Phase II, Single-Arm, Open-Label, Multicenter Study to Evaluate the Efficacy and Safety of P276-00, a Cyclin-Dependent Kinase Inhibitor, in Patients With Relapsed or Refractory Mantle Cell Lymphoma, *Clin. Lymphoma, Myeloma Leuk.*, 15 (2015) 392-397.
- [34] K.K. Murthi, M. Dubay, C. McClure, L. Brizuela, M.D. Boisclair, P.J. Worland, M.M. Mansuri, K. Pal, Structure-activity relationship studies of flavopiridol analogues, *Bioorg. Med. Chem. Lett.*, 10 (2000) 1037-1041.

- [35] K.S. Kim, J.S. Sack, J.S. Tokarski, L. Qian, S.T. Chao, L. Leith, Y.F. Kelly, R.N. Misra, J.T. Hunt, S.D. Kimball, W.G. Humphreys, B.S. Wautlet, J.G. Mulheron, K.R. Webster, Thio- and Oxoflavopiridols, Cyclin-Dependent Kinase 1-Selective Inhibitors: Synthesis and Biological Effects, *J. Med. Chem.*, 43 (2000) 4126-4134.
- [36] J. Schoepfer, H. Fretz, B. Chaudhuri, L. Muller, E. Seeber, L. Meijer, O. Lozach, E. Vangrevelinghe, P. Furet, Structure-Based Design and Synthesis of 2-Benzylidene-benzofuran-3-ones as Flavopiridol Mimics, *J. Med. Chem.*, 45 (2002) 1741-1747.
- [37] K.S. Joshi, M.J. Rathos, R.D. Joshi, M. Sivakumar, M. Mascarenhas, S. Kamble, B. Lal, S. Sharma, In vitro antitumor properties of a novel cyclin-dependent kinase inhibitor, P276-00, *Mol. Cancer Ther.*, 6 (2007) 918-925.
- [38] J. Czech, D. Hoffmann, R. Naik, H.H. Sedlacek, Antitumoral activity of flavone L-86-8275., *Int. J. Oncol.*, 6 (1995) 31-36.
- [39] A.C. Tabaka, K.K. Murthi, K. Pal, C.A. Teleha, Application of Modified Flavone Closure for the Preparation of Racemic L86-8275, *Org. Process Res. Dev.*, 3 (1999) 256-259.
- [40] A. Bruneau, M. Roche, A. Hamze, J.-D. Brion, M. Alami, S. Messaoudi, Stereoretentive Palladium-Catalyzed Arylation, Alkenylation, and Alkynylation of 1-Thiosugars and Thiols Using Aminobiphenyl Palladacycle Precatalyst at Room Temperature, *Chem. – A Eur. J.*, 21 (2015) 8375-8379.
- [41] N. Probst, R. Lartia, O. Théry, M. Alami, E. Defrancq, S. Messaoudi, Efficient Buchwald–Hartwig–Migita Cross-Coupling for DNA Thioglycoconjugation, *Chem. Eur. J.*, 24 (2018) 1795-1800.
- [42] D. Montoir, M. Amoura, Z.E.A. Ababsa, T.M. Vishwanatha, E. Yen-Pon, V. Robert, M. Beltramo, V. Piller, M. Alami, V. Aucagne, S. Messaoudi, Synthesis of aryl-thioglycopeptides through chemoselective Pd-mediated conjugation, *Chem. Sci.*, 9 (2018) 8753-8759.
- [43] H. Ma, N.A. Seebacher, F.J. Hornicek, Z. Duan, Cyclin-dependent kinase 9 (CDK9) is a novel prognostic marker and therapeutic target in osteosarcoma, *EBioMedicine*, 39 (2019) 182-193.
- [44] F. Lo Monte, T. Kramer, J. Gu, U.R. Anumala, L. Marinelli, V. La Pietra, E. Novellino, B. Franco, D. Demedts, F. Van Leuven, A. Fuertes, J.M. Dominguez, B. Plotkin, H. Eldar-Finkelman, B. Schmidt, Identification of Glycogen Synthase Kinase-3 Inhibitors with a Selective Sting for Glycogen Synthase Kinase-3 α , *J. Med. Chem.*, 55 (2012) 4407-4424.
- [45] N. Floyd, B. Vijayakrishnan, J.R. Koeppe, B.G. Davis, Thiyl Glycosylation of Olefinic Proteins: S-Linked Glycoconjugate Synthesis, *Angew. Chem., Int. Ed.*, 48 (2009) 7798-7802.
- [46] D.P. Gamblin, P. Garnier, S. van Kasteren, N.J. Oldham, A.J. Fairbanks, B.G. Davis, Glyco-SeS: Selenenylsulfide-Mediated Protein Glycoconjugation—A New Strategy in Post-Translational Modification, *Angew. Chem., Int. Ed.*, 43 (2004) 828-833.
- [47] N.C. Bruno, M.T. Tudge, S.L. Buchwald, Design and preparation of new palladium precatalysts for C–C and C–N cross-coupling reactions, *Chem. Sci.*, 4 (2013) 916-920.
- [48] D.W. Siemann, D.J. Chaplin, P.A. Walicke, A review and update of the current status of the vasculature-disabling agent combretastatin-A4 phosphate (CA4P), *Expert Opin. Invest. Drugs*, 18 (2009) 189-197.
- [49] T.-N.-D. Nguyen, O. Feizbakhsh, E. Sfecci, B. Baratte, C. Delehouzé, A. Garcia, C. Moulin, P. Colas, S. Ruchaud, M. Mehiri, S. Bach, Kinase-Based Screening of Marine Natural Extracts Leads to the Identification of a Cytotoxic High Molecular Weight Metabolite from the Mediterranean Sponge *Crambe tailliezi*, *Mar. Drugs*, 17 (2019) 569.